

2018

A Kernel-based embedding method and convergence analysis for surfaces PDEs

Ka Chun Cheung

Hong Kong Baptist University, kccheung@astri.org

Leevan Ling

Hong Kong Baptist University, lling@hkbu.edu.hk

This document is the authors' final version of the published article.

Link to published article: <http://dx.doi.org/10.1137/16M1080410>

APA Citation

Cheung, K., & Ling, L. (2018). A Kernel-based embedding method and convergence analysis for surfaces PDEs. *SIAM Journal on Numerical Analysis*, 40 (1), A266-A287. <https://doi.org/10.1137/16M1080410>

This Journal Article is brought to you for free and open access by HKBU Institutional Repository. It has been accepted for inclusion in HKBU Staff Publication by an authorized administrator of HKBU Institutional Repository. For more information, please contact repository@hkbu.edu.hk.

A KERNEL-BASED EMBEDDING METHOD AND CONVERGENCE ANALYSIS FOR SURFACES PDES

KA CHUN CHEUNG* AND LEEVAN LING†

Abstract. We analyze a least-squares strong-form kernel collocation formulation for solving second order elliptic PDEs on smooth, connected and compact surfaces with bounded geometry. The methods do not require any partial derivatives of surface normal vectors or metric. Based on some standard smoothness assumptions for high order convergence, we provide the sufficient denseness conditions on the collocation points to ensure the methods are convergent. Besides of some convergence verifications, we also simulate some reaction-diffusion equations to exhibit the pattern formations.

Key words. Meshfree method, Kansa method, radial basis function, overdetermined collocation, narrow-band method.

AMS subject classifications. 65D15, 65N35, 41A63.

1. Introduction. The unsymmetric strong-form meshfree collocation method, a.k.a. the Kansa method [21, 22], which is already popular for solving PDEs of various kinds, is simple to implement. It also handles scattered data and time-varying discretization with ease, which is one of the many reasons for its popularity. Because of its high flexibility, the number of successful applications of the Kansa method has grown dramatically since the method was proposed in 1990. Theories of the Kansa method are rather limited. However, one certainty is that its original exactly-determined formulation cannot even guarantee solvability [20]. Yet, this does not make researchers abandon the Kansa method. Alternatively, many variations of modified Kansa methods and rule-of-thumbs have been suggested and numerically studied. It is obvious that the theoretical development does not measure up to the popularity of the Kansa method. Recently, we proved an optimal \mathcal{H}^2 -convergence of a class of least-squares Kansa methods for solving general second order elliptic problems with Dirichlet boundary conditions, see [9]. In this paper, we aim to take a step forward by applying a Kansa method to PDEs on surfaces. We consider general second order strongly elliptic partial differential equations

$$\mathcal{L}_S u = f \quad \text{on } \mathcal{S} \subset \mathbb{R}^d, \quad (1.1)$$

where the surface differential operator $\mathcal{L}_S : \mathcal{H}^m(\mathcal{S}) \rightarrow \mathcal{H}^{m-2}(\mathcal{S})$ has $\mathcal{W}_\infty^m(\mathcal{S})$ -bounded coefficients and is in the form of:

$$\mathcal{L}_S := -a\Delta_S + \mathbf{b} \cdot \nabla_S + c, \quad (1.2)$$

on some smooth, connected, and compact surface \mathcal{S} with bounded geometry (i.e., \mathcal{S} is complete) and $\dim(\mathcal{S}) = d-1$. Let $\hat{\mathbf{n}} = \hat{\mathbf{n}}(\mathbf{p})$ denote the unit outward normal vector at $\mathbf{p} \in \mathcal{S}$. Then the surface gradient ∇_S and the Laplace-Beltrami Δ_S operators (a.k.a. the surface Laplacian) in (1.2) can be defined in terms of the standard Euclidean gradient ∇ and Laplacian Δ operators for \mathbb{R}^d via projections:

$$\nabla_S := (I - \mathbf{nn}^T)\nabla \quad \text{and} \quad \Delta_S := \nabla_S \cdot \nabla_S, \quad (1.3)$$

*Department of Mathematics, Hong Kong Baptist University, Kowloon Tong, Hong Kong & ASTRI Hong Kong Applied Science and Technology Research Institute Company Limited. (kccheung@astri.org)

†Department of Mathematics, Hong Kong Baptist University, Kowloon Tong, Hong Kong. (lling@hkbu.edu.hk)

where I is the identity operator. Typically, numerical methods for solving (1.2) can be classified into two types: intrinsic and embedding. The former requires some parametrization with local coordinates and discretization of the surface differential operator based on surface mesh. The latter methods solve the PDEs in some embedding spaces and is more related to the framework of meshfree method.

We are interested in casting some variants of Kansa methods to obtain an embedding method. Ruuth et al. [33] proposed the closest point method for surface PDEs by the closest point (or constant-along-normal) mapping. Once embedded, one can simply replace the surface gradient and the Laplacian-Beltrami operators by the standard ones in Euclidean spaces. The embedded PDE can then be solved by available numerical solvers developed in Euclidean space. In the same article, the standard finite difference method was used for discretization with second order accuracy. Carefully implemented interpolation between points on the surface and computational grids were required for efficiency; further speed up can be achieved by multigrid [7]. Once the surface differential operator is appropriately discretized, it can be used to solve eigenvalue problems on surfaces [24]. When combined with the method-of-lines or any semi-discrete approach [23, 25, 31], numerical methods for (1.2) can be extended to time-dependent surface PDEs.

The orthogonal gradients method [29] is a meshfree extension of the closest-point method. It uses data points orthogonal to the surface and, by construction, all off-surface data points are in the normal direction of some data points on the surface. Hence, they have identical function values under the closest point mapping. In this setting, one must work with irregular data points and this is where meshfree methods come into the play. To discretize the surface operator, one can work within the embedding space and use a meshfree finite difference approach (for Euclidean spaces) [39, 41] in order to approximate the surface differential operator. It is shown in [8] that combining the ideas of closest point and meshfree methods can successfully handle PDEs on surfaces with corners.

Another meshfree approach is to directly project kernel-based approximants onto the surface, see [13], to discretize surface operators at nodal points. Instead of the closest point approach, this approach works with the projection operator $I - \hat{\mathbf{n}}\hat{\mathbf{n}}^T$ arisen naturally from the definitions in (1.3). By combining surface projections with the meshfree interpolant and its derivatives carefully, full convergence theories can be found in the same article. Having the meshfree interpolant as the key player, the method is in a symmetric setting and one cannot collocate freely.

The development of meshfree methods for surface PDEs is similar to its \mathbb{R}^d counterpart. This paper aims to extend the meshfree theories for surface PDEs from symmetric to unsymmetric settings, which yield methods that is similar to the orthogonal gradients method [29] but has more flexibility in the positioning of the off-surface points. In Section 2, a brief discussion on the closest point embedding technique and the associated embedding conditions are given. In Section 3, we build up a series of the meshfree theories concerning meshfree method in the embedding spaces. In particular, we prove a regularity estimate, a sampling inequality and an inverse inequality in order to obtain a stability estimate, which gives rise to our proposed kernel-based embedding method. The main challenge here is to connect trial functions defined in the embedded spaces to the surface. All the results are of some hybrid types in the sense that both the surface and the embedded spaces are involved in these inequalities. In Section 4, we provide the implementation details and a convergence estimate of our proposed method. Readers can see that the original orthogonal gradients methods use

either the stability or embedding conditions in our analysis. In Section 5, we present various numerical demonstrations concerning the convergence behaviour of our proposed method. Then, by some three-dimensional pattern formations, we demonstrate that the proposed method is numerically stable to deal with time-dependent PDEs.

2. Embedding conditions. Sobolev spaces on complete surfaces with bounded geometry [34] can be defined by $\mathcal{H}^m(\mathcal{S}) := (I - \Delta_{\mathcal{S}})^{-m/2} L^2(\mathcal{S})$. For $m \in \mathbb{N}$, $\mathcal{H}^m(\mathcal{S})$ is norm equivalent to the Sobolev space containing all L^2 functions on \mathcal{S} with bounded covariant derivatives up to order m , see [40]. Instead of using covariant derivatives, we can equivalently characterize the space by localization with an atlas of geodesic normal charts $\{(\mathcal{U}_i, \varphi_i)\}$ and a subordinate partition of unity χ_i , see [19, Prop.2.2], which is the common definition used in meshfree theories on manifolds, also see [12].

We consider smooth, connected and compact Riemannian manifolds with sufficient smoothness and differentiability. A surface \mathcal{S} is of smoothness class \mathcal{C}^m if there is a collection of charts $\{(\mathcal{U}_i, \varphi_i) \mid i \in \mathbb{N}\}$, a.k.a. an atlas of \mathcal{S} , so that $\mathcal{S} = \bigcup_i \mathcal{U}_i$ and $\varphi_i : \mathcal{U}_i \rightarrow \varphi_i(\mathcal{U}_i) \subset \mathbb{R}^{\dim(\mathcal{S})}$ is a homeomorphism such that $\varphi_i \circ \varphi_j^{-1}$ is of class \mathcal{C}^m for all $i, j \in \mathbb{N}$. The associated norms are defined by

$$\|u\|_{\mathcal{H}^m(\mathcal{S})} := \sum_{|\alpha| \leq m} \sum_{i \in \mathbb{N}} \left\| D^\alpha ((\chi_i u) \circ \varphi_i^{-1}) \right\|_{L^2(\varphi_i(\mathcal{U}_i))}, \quad (2.1)$$

where D^α is the standard multi-index differential operator in $\mathbb{R}^{\dim(\mathcal{S})}$. The norm in (2.1) clearly depends on the selection of $\{(\mathcal{U}_i, \varphi_i, \chi_i) \mid i \in \mathbb{N}\}$ but is norm equivalent to the norm generated by any other selection. Without loss of generality, any atlas dependency is considered as \mathcal{S} dependent in our forthcoming analysis. By assuming \mathcal{S} compact, any atlas of \mathcal{S} has a finite number of charts. As a result, \mathcal{S} is complete. The Hopf-Rinow Theorem then ensures that we can measure the distance between any two points of \mathcal{S} by the associated geodesic. Compactness of \mathcal{S} also guarantees bounded geometry so that every covariant derivative of the Riemannian curvature tensor is uniformly bounded. In particular, our analysis requires certain uniform boundedness of the Jacobian $J(\hat{\mathbf{n}})$ of the normal vector of \mathcal{S} and satisfy some local geometric properties in [18, Asm.2.1] similar to standard cone conditions in \mathbb{R}^d .

We assume the function f in (1.1) is sufficiently smooth to admit a classical solution, which we denote by $u_{\mathcal{S}}^*$ throughout the paper. Our method is built upon the constant-along-normal property. To begin, we take a detour to the finite difference based closest point method [33] and its meshfree extension [29]. The key idea we need from them is the closest point mapping cp , which maps each “nearby” point $\mathbf{x} \in \mathbb{R}^d$ onto the surface $\text{cp}(\mathbf{x}) \in \mathcal{S}$ so that $\text{cp}(\mathbf{x}) = \arg \inf_{\mathbf{p} \in \mathcal{S}} \|\mathbf{p} - \mathbf{x}\|_{\ell^2(\mathbb{R}^d)}$. For any \mathcal{S} of class \mathcal{C}^{m+1} , there exists a fixed domain

$$\Sigma := \left\{ \mathbf{x} \in \mathbb{R}^d : \inf_{\mathbf{p} \in \mathcal{S}} \|\mathbf{p} - \mathbf{x}\|_{\ell^2(\mathbb{R}^d)} < \varepsilon_0 < \min(1, \varepsilon_{\text{cp}, m}) \right\} \quad (2.2)$$

for some constant $\varepsilon_{\text{cp}, m}$ depending only on \mathcal{S} and m such that $u_{\mathcal{S}} \circ \text{cp} \in \mathcal{H}^m(\Sigma)$ for all $u_{\mathcal{S}} \in \mathcal{H}^m(\mathcal{S})$, see [7]. Our goal is to properly “embed” the surface PDE in (1.1) to some narrow-band domains in Σ and work with another PDE operator in the form of

$$\mathcal{L}_E := -a_E \Delta + \mathbf{b}_E \cdot \nabla + c_E \quad \text{in } \Sigma, \quad (2.3)$$

in which all incidents of $\nabla_{\mathcal{S}}$ are replaced by the Euclidean gradient operator ∇ . All coefficients in (2.3) are cp -extensions of those in (1.2), i.e. $a_E = a \circ \text{cp}$ and etc for all $\mathbf{x} \in \Sigma$.

Generally speaking, the surface operator in (1.2) and Euclidean operator in (2.3) are different; however, the two operators coincide for a certain class of functions. In [29], it was proposed that functions defined on Σ with sufficient smoothness and satisfying embedding conditions $n \cdot \nabla u = 0$ and $(\hat{\mathbf{n}} \cdot \nabla)(\hat{\mathbf{n}} \cdot \nabla)u = 0$ have the desired $\mathcal{L}_{\mathcal{S}}u = (\mathcal{L}_E u)|_{\mathcal{S}}$ property for $\mathcal{S} \subset \mathbb{R}^3$. Note, in the latter condition, partial derivatives of the surface normal $\hat{\mathbf{n}}$ are required. In the following theorem, we prove some other embedding conditions that only require $\hat{\mathbf{n}}$ but not its derivatives, which allows us to develop methods working on point cloud on \mathcal{S} without an explicit formula for $\hat{\mathbf{n}}$.

THEOREM 2.1 (Embedding Conditions). *Let $\mathcal{S} \subset \mathbb{R}^d$ be a codimension one \mathcal{C}^3 -smooth, connected and compact surface with well-defined normal $\hat{\mathbf{n}} = \hat{\mathbf{n}}(\mathbf{p})$ for all $\mathbf{p} \in \mathcal{S}$. Let $u \in \mathcal{C}^2(\Sigma) \cap \mathcal{H}^{2+\frac{1}{2}}(\Sigma)$ be an extension of $u_{\mathcal{S}} \in \mathcal{H}^2(\mathcal{S})$ with $u|_{\mathcal{S}} = u_{\mathcal{S}}$. Then,*

$$\nabla_{\mathcal{S}}u := \nabla u - \hat{\mathbf{n}}\partial_{\hat{\mathbf{n}}}u \quad \text{and} \quad \Delta_{\mathcal{S}}u := \Delta u - H_{\mathcal{S}}\partial_{\hat{\mathbf{n}}}u - \partial_{\hat{\mathbf{n}}}^{(2)}u \quad \text{on } \mathcal{S}, \quad (2.4)$$

where $\partial_{\hat{\mathbf{n}}}u := \hat{\mathbf{n}}^T \nabla u$, $\partial_{\hat{\mathbf{n}}}^{(2)}u := \hat{\mathbf{n}}^T J(\nabla u)\hat{\mathbf{n}}$ and $H_{\mathcal{S}}(\mathbf{p}) = \text{tr}\left(J(\hat{\mathbf{n}})(I - \hat{\mathbf{n}}\hat{\mathbf{n}}^T)\right)$, which is d times the mean curvature of \mathcal{S} at \mathbf{p} , defined using the Jacobian operator J in Euclidean space. In particular, for any second order differential operator in the form of (1.2), if u satisfies the embedding conditions

$$\partial_{\hat{\mathbf{n}}}u = 0 \quad \text{and} \quad \partial_{\hat{\mathbf{n}}}^{(2)}u = 0 \quad \text{on } \mathcal{S}, \quad (2.5)$$

then $\mathcal{L}_{\mathcal{S}}u_{\mathcal{S}} = \mathcal{L}_E u$ on \mathcal{S} .

Proof. Since $\nabla_{\mathcal{S}}u = \nabla u - (\hat{\mathbf{n}}^T \nabla u)\hat{\mathbf{n}}$ for sufficiently smooth u , the two gradient operators coincide on \mathcal{S} as long as $\hat{\mathbf{n}}^T \nabla u = 0$. Consider the surface Laplacian operator defined as

$$\begin{aligned} \Delta_{\mathcal{S}}u &:= \nabla_{\mathcal{S}} \cdot \nabla_{\mathcal{S}}u = (I - \hat{\mathbf{n}}\hat{\mathbf{n}}^T)\nabla \cdot (I - \hat{\mathbf{n}}\hat{\mathbf{n}}^T)\nabla u \\ &= \Delta u - (\hat{\mathbf{n}}\hat{\mathbf{n}}^T \nabla) \cdot \nabla u - (I - \hat{\mathbf{n}}\hat{\mathbf{n}}^T)\nabla \cdot (\hat{\mathbf{n}}\hat{\mathbf{n}}^T \nabla u). \end{aligned} \quad (2.6)$$

It can be verified easily by the Einstein summation notation that

$$(A\nabla) \cdot (B\nabla u) = A_{ij}(B_{ik}u_{,k})_{,j} = \text{tr}((B_{ik}u_{,k})_{,j}A_{j\ell}^T) = \text{tr}(J(B\nabla u)A^T). \quad (2.7)$$

Putting $A = \hat{\mathbf{n}}\hat{\mathbf{n}}^T$ and $B = I$ in (2.7), we have

$$(\hat{\mathbf{n}}\hat{\mathbf{n}}^T \nabla) \cdot \nabla u = \text{tr}(J(\nabla u)\hat{\mathbf{n}}\hat{\mathbf{n}}^T) = \text{tr}(u_{,ij}\hat{\mathbf{n}}_j\hat{\mathbf{n}}_i) = \hat{\mathbf{n}}^T J(\nabla u)\hat{\mathbf{n}},$$

which yields one of the embedding conditions u must satisfy. Now, we simplify the last term in (2.6) in order to eliminate all the derivatives of $\hat{\mathbf{n}}$ from the other embedding condition. Using (2.7), we have

$$\begin{aligned} (I - \hat{\mathbf{n}}\hat{\mathbf{n}}^T)\nabla \cdot (\hat{\mathbf{n}}\hat{\mathbf{n}}^T \nabla u) &= \text{tr}\left(J(\hat{\mathbf{n}}\hat{\mathbf{n}}^T \nabla u)(I - \hat{\mathbf{n}}\hat{\mathbf{n}}^T)\right) \\ &= \text{tr}\left(J(\hat{\mathbf{n}}\hat{\mathbf{n}}^T \nabla u)\right) - \text{tr}\left(J(\hat{\mathbf{n}}\hat{\mathbf{n}}^T \nabla u)\hat{\mathbf{n}}\hat{\mathbf{n}}^T\right). \end{aligned}$$

Carrying on with more arithmetic operations, we can show that

$$\begin{aligned} \text{tr}\left(J(\hat{\mathbf{n}}\hat{\mathbf{n}}^T \nabla u)\right) &= (\hat{\mathbf{n}}_i\hat{\mathbf{n}}_j u_{,j})_{,i} = (\hat{\mathbf{n}}_{i,i}\hat{\mathbf{n}}_j + \hat{\mathbf{n}}_i\hat{\mathbf{n}}_{j,i})u_{,j} + \hat{\mathbf{n}}_i\hat{\mathbf{n}}_j u_{,ij} \\ &= \text{tr}(J(\hat{\mathbf{n}}))\hat{\mathbf{n}}^T \nabla u + \hat{\mathbf{n}}^T J(\hat{\mathbf{n}})\nabla u + \hat{\mathbf{n}}^T J(\nabla u)\hat{\mathbf{n}}, \end{aligned}$$

and $\text{tr} \left(J(\hat{\mathbf{n}}\hat{\mathbf{n}}^T \nabla u) \hat{\mathbf{n}}\hat{\mathbf{n}}^T \right) = \text{tr} \left(J(\hat{\mathbf{n}})\hat{\mathbf{n}}\hat{\mathbf{n}}^T \right) \hat{\mathbf{n}}^T \nabla u + \hat{\mathbf{n}}^T J(\hat{\mathbf{n}}) \nabla u + \hat{\mathbf{n}}^T J(\nabla u) \hat{\mathbf{n}}$. After cancellation, we obtain $(I - \hat{\mathbf{n}}\hat{\mathbf{n}}^T) \nabla \cdot (\hat{\mathbf{n}}\hat{\mathbf{n}}^T \nabla u) = \text{tr} \left(J(\hat{\mathbf{n}})(I - \hat{\mathbf{n}}\hat{\mathbf{n}}^T) \right) (\hat{\mathbf{n}}^T \nabla u)$. Altogether, the equalities in (2.4) hold for any $\mathbf{p} \in \mathcal{S}$ and (2.5) follows immediately. \square

COROLLARY 2.2. *Suppose all assumptions in Theorem 2.1 hold. Then there exist some constant C depending only on \mathcal{S} and $\mathcal{L}_{\mathcal{S}}$ such that*

$$\|\mathcal{L}_{\mathcal{S}} u_{\mathcal{S}}\|_{\ell^2(X)}^2 \leq C \left(\|\mathcal{L}_{E} u\|_{\ell^2(X)}^2 + \|\partial_{\hat{\mathbf{n}}} u\|_{\ell^2(X)}^2 + \|\partial_{\hat{\mathbf{n}}}^{(2)} u\|_{\ell^2(X)}^2 \right)$$

holds for any discrete set $X \subset \mathcal{S}$.

3. Stability estimates of embedded PDEs. Let $\text{sgn}_{\mathcal{S}}$ be an indicator function so that $\text{sgn}_{\mathcal{S}}(\mathbf{x}) = -1$ (or $+1$) if \mathbf{x} is located inside (or outside) of the closed surface \mathcal{S} , and $\text{sgn}_{\mathcal{S}}(\mathbf{p}) = 0$ for all $\mathbf{p} \in \mathcal{S}$. We define a sequence of narrow-band domains by

$$\Omega_{\delta} = \{\mathbf{x} \in \mathbb{R}^d : \|\mathbf{x} - \mathbf{p}\|_{\ell_2(\mathbb{R}^d)} < \delta \text{ for some } \mathbf{p} \in \mathcal{S}\}, \quad (3.1)$$

and parallel surfaces

$$\mathcal{S}_{\delta} = \{\mathbf{x} \in \mathbb{R}^d : \text{sgn}_{\mathcal{S}}(\mathbf{x}) \|\mathbf{x} - \mathbf{p}\|_{\ell_2(\mathbb{R}^d)} = \delta \text{ for some } \mathbf{p} \in \mathcal{S}\}, \quad (3.2)$$

with respect to some $\delta \in \mathbb{R}$. To cp-embed the surface PDEs into these Ω_{δ} , we prove a norm equivalency for Sobolev norms on \mathcal{S} and Ω_{δ} so that we can go between any function on \mathcal{S} and its cp-extension.

LEMMA 3.1. *Suppose \mathcal{S} is of class \mathcal{C}^{m+1} with $m \geq 0$ and let $\Omega_{\delta} \subset \Sigma$ be defined as in (3.1) with sufficiently small δ with respects to \mathcal{S} . Then there exists some constants C_1 and C_2 depending only on \mathcal{S} and k such that*

$$C_1 \delta^{1/2} \|u\|_{\mathcal{H}^k(\mathcal{S})} \leq \|u \circ \text{cp}\|_{\mathcal{H}^k(\Omega_{\delta})} \leq C_2 \delta^{1/2} \|u\|_{\mathcal{H}^k(\mathcal{S})}, \quad 0 \leq k \leq m$$

holds for all $u \in \mathcal{H}^m(\mathcal{S})$.

Proof. With $u_{\mathcal{S}} \in \mathcal{H}^m(\mathcal{S})$ for some \mathcal{C}^{m+1} surfaces, we know that $u_{\mathcal{S}} \circ \text{cp} \in \mathcal{H}^m(\Sigma)$ for all $u \in \mathcal{H}^m(\mathcal{S})$ and all Sobolev norms in the lemma are well-defined. Let $\{(\mathcal{U}_i, \varphi_i)\}_{i=1}^N$ be the selected atlas for \mathcal{S} and χ_i the associated subordinate partition of unity.

For any fixed $t > 0$, define a bijection from the surface to its t -parallel surface by $T_t : \mathcal{S} \mapsto \mathcal{S}_t$ such that $T_t(\mathbf{p}) := \mathbf{p} + t\hat{\mathbf{n}}(\mathbf{p})$ for any $\mathbf{p} \in \mathcal{S}$. Note that the cp operator is a left inverse of T_t such that $\text{cp} \circ T_t = \text{id}$. Now, we define an atlas $\{(\mathcal{U}_i^t, \varphi_i^t)\}_{i=1}^N$ and a partition of unity χ_i^t for \mathcal{S}_t based on the one for \mathcal{S} . In particular, let $\mathcal{U}_i^t = T_t(\mathcal{U}_i)$ and $\varphi_i^t = \varphi_i \circ T_t^{-1}$. Moreover, $\chi_i^t = \chi_i \circ T_t^{-1}$ is a partition of unity for \mathcal{S}_t subordinated to $\{\mathcal{U}_i^t\}$. Then, the Sobolev norm on the parallel surface \mathcal{S}_t can be defined by (2.1) and we have

$$\begin{aligned} \|u\|_{\mathcal{H}^k(\mathcal{S}_t)}^2 &:= \sum_{i \in \mathbb{N}} \|(\chi_i^t u) \circ (\varphi_i^t)^{-1}\|_{\mathcal{H}^k(\varphi_i^t(\mathcal{U}_i^t))}^2 \\ &= \sum_{i \in \mathbb{N}} \sum_{|\alpha| \leq k} \int_{\varphi_i \circ T_t^{-1}(\mathcal{U}_i^t)} \left| D^{\alpha} \left(((\chi_i \circ T_t^{-1})u) \circ (\varphi_i \circ T_t^{-1})^{-1} \right) \right|^2 d\boldsymbol{\theta} \\ &= \sum_{|\alpha| \leq k} \sum_{i \in \mathbb{N}} \int_{\varphi_i(\mathcal{U}_i)} \left| D^{\alpha} \left(((\chi_i \circ T_t^{-1})u) \circ (T_t \circ \varphi_i^{-1}) \right) \right|^2 d\boldsymbol{\theta} \\ &= \sum_{|\alpha| \leq k} \sum_{i \in \mathbb{N}} \int_{\varphi_i(\mathcal{U}_i)} \left| D^{\alpha} \left((\chi_i(u \circ T_t)) \circ \varphi_i^{-1} \right) \right|^2 d\boldsymbol{\theta} =: \|u \circ T_t\|_{\mathcal{H}^k(\mathcal{S})}^2, \end{aligned}$$

or equivalently, $\|u\|_{\mathcal{H}^k(\mathcal{S})}^2 = \|u \circ T_t^{-1}\|_{\mathcal{H}^k(\mathcal{S}_t)}^2 = \|u \circ cp\|_{\mathcal{H}^k(\mathcal{S}_t)}^2$ for $k \leq m$. Using the coarea formula, we can obtain

$$\begin{aligned}
\|u \circ cp\|_{\mathcal{H}^k(\Omega_\delta)}^2 &= \sum_{|\alpha| \leq k} \int_{-\delta}^{\delta} \int_{\mathcal{S}_t} \left| D^\alpha \left(\sum_{i \in \mathbb{N}} \chi_i^t(u \circ cp) \right) \right|^2 d\mathbf{x} dt \\
&\leq \sum_{|\alpha| \leq k} \sum_{i \in \mathbb{N}} \int_{-\delta}^{\delta} \int_{\mathcal{U}_i^t} \left| D^\alpha (\chi_i^t(u \circ cp)) \right|^2 d\mathbf{x} dt \\
&= \sum_{|\alpha| \leq k} \sum_{i \in \mathbb{N}} \int_{-\delta}^{\delta} \int_{\varphi_i^t(\mathcal{U}_i^t)} \left| D^\alpha ((\chi_i^t(u \circ cp))) \right|^2 \left| \det(J((\varphi_i^t)^{-1})) \right| d\boldsymbol{\theta} dt \\
&\leq C_{\mathcal{S},k} \left(\sup_{i \in \mathbb{N}} \sup_{\boldsymbol{\theta} \in \varphi_i^t(\mathcal{U}_i^t)} \left| \det(J((\varphi_i^t)^{-1}\boldsymbol{\theta})) \right| \right) \int_{-\delta}^{\delta} \|u \circ cp\|_{\mathcal{H}^k(\mathcal{S}_t)}^2 dt \\
&= 2\delta C_{\mathcal{S},k} \left(\sup_{\mathbf{p} \in \mathcal{S}} \left| \det(J(T_t(\mathbf{p}))) \right| \right) \|u\|_{\mathcal{H}^k(\mathcal{S})}^2.
\end{aligned}$$

By considering the characteristic polynomial of $\det(t^{-1}I + J(\hat{\mathbf{n}}))$, whose coefficients $\lambda_i(\mathbf{p})$ can be written in terms of traces of powers of $J(\hat{\mathbf{n}}(\mathbf{p}))$, we have

$$\begin{aligned}
\det(J(T_t(\mathbf{p}))) &= \det(I + tJ(\hat{\mathbf{n}})) = t^d \det(t^{-1}I + J(\hat{\mathbf{n}})) \\
&= t^d \cdot (-1)^d \left(t^{-d} + \sum_{i=1}^d \lambda_i t^{i-d} \right) = (-1)^d \left(1 + \sum_{i=1}^d \lambda_i t^i \right).
\end{aligned}$$

Since \mathcal{S} has bounded geometry, all (covariant and partial) derivatives of $\hat{\mathbf{n}}$ are bounded. If t is small enough in terms of λ_i , which solely depends on \mathcal{S} , then there exist some constants $0 \leq c_{\mathcal{S}} \leq C_{\mathcal{S}} < 1/2$ so that

$$1 - c_{\mathcal{S}} \leq \left| \det(J(T_t(\mathbf{p}))) \right| \leq 1 + C_{\mathcal{S}} \quad \text{for all } \mathbf{p} \in \mathcal{S}. \quad (3.3)$$

To obtain the lower bound, consider

$$\begin{aligned}
\|u\|_{\mathcal{H}^k(\mathcal{S})}^2 &= \|u \circ cp\|_{\mathcal{H}^k(\mathcal{S}_t)}^2 = \sum_{i \in \mathbb{N}} \|(\chi_i^t(u \circ cp)) \circ (\varphi_i^t)^{-1}\|_{\mathcal{H}^k(\varphi_i^t(\mathcal{U}_i^t))}^2 \\
&= \sum_{|\alpha| \leq k} \sum_{i \in \mathbb{N}} \int_{\varphi_i^t(\mathcal{U}_i^t)} \left| D^\alpha ((\chi_i^t(u \circ cp)) \circ (\varphi_i^t)^{-1}) \right|^2 d\boldsymbol{\theta} \\
&= \sum_{|\alpha| \leq k} \sum_{i \in \mathbb{N}} \int_{\mathcal{U}_i^t} \left| D^\alpha (\chi_i^t(u \circ cp)) \right|^2 \left| \det(J(\varphi_i^t)) \right| d\mathbf{x} \\
&\leq C_{\mathcal{S},k} \sum_{|\alpha| \leq k} \int_{\mathcal{S}_t} \sum_{i \in \mathbb{N}} \left| \sum_{|\beta| \leq |\alpha|} \binom{\alpha}{\beta} D^\beta \chi_i^t D^{\alpha-\beta}(u \circ cp) \right|^2 d\mathbf{x} \\
&\leq C_{\mathcal{S},k} \left(\sup_{i \in \mathbb{N}} \sup_{|\alpha| \leq k} \left| D^\alpha \chi_i^t \right| \right) \sum_{|\alpha| \leq k} \int_{\mathcal{S}_t} \left| D^\alpha (u \circ cp) \right|^2 d\mathbf{x}.
\end{aligned}$$

Since \mathcal{S} has bounded geometry, the supremum of $|D^\alpha \chi_i^t|$ is bounded for $k \leq m+1$, see [38, Thm.2.13]. We can now complete the proof by integrating both sides with

respect to t and show that

$$2\delta \|u\|_{\mathcal{H}^k(\mathcal{S})}^2 \leq C'_{\mathcal{S},k} \sum_{|\alpha| \leq k} \int_{-\delta}^{\delta} \int_{\mathcal{S}_t} |D^\alpha(u \circ cp)|^2 d\mathbf{x} dt = C'_{\mathcal{S},k} \|u\|_{\mathcal{H}^k(\Omega_\delta)}^2.$$

Since $k \leq m$, we can bound all constants $C'_{\mathcal{S},k}$ by one that is independent of k for simplicity. \square

With Lemma 3.1, we can develop a regularity estimate for the surface PDE in (1.1). Unlike the typical ones, this estimate uses a norm in Ω_δ instead of on \mathcal{S} to bound a norm on \mathcal{S} .

THEOREM 3.2 (Regularity). *Suppose \mathcal{S} is of class \mathcal{C}^{m+1} for some $m \geq 2$ and the narrow-band domain $\Omega_\delta \subset \Sigma$ has a sufficiently small δ so that Lemma 3.1 holds. Then there exists a constant C depending only on \mathcal{S} such that*

$$\|u\|_{\mathcal{H}^k(\mathcal{S})} \leq C\delta^{-1/2} \|\mathcal{L}_E(u \circ cp)\|_{\mathcal{H}^{k-2}(\Omega_\delta)}, \quad 2 \leq k \leq m \quad (3.4)$$

for all $u \in \mathcal{H}^m(\mathcal{S})$.

Proof. Considering a regularity estimate for second-order linear elliptic PDEs on some smooth domain Ω_δ subject to Neumann boundary conditions, viz.,

$$\|w\|_{\mathcal{H}^k(\Omega_\delta)} \leq C_{\Omega_\delta} \left(\|\mathcal{L}_E w\|_{\mathcal{H}^{k-2}(\Omega_\delta)} + \|\partial_{\mathbf{n}} w\|_{\mathcal{H}^{k-3/2}(\partial\Omega_\delta)} \right) \quad \text{for all } w \in \mathcal{H}^m(\Omega_\delta).$$

The regularity constant C_{Ω_δ} here depends on some open ball bounding Ω_δ . Hence, it can be bounded by some $C_\Sigma = C_{\mathcal{S}}$ instead. Since the function $w = u \circ cp$ satisfies this regularity estimate for any $u \in \mathcal{H}^m(\mathcal{S})$, inequality (3.4) follows immediately Lemma (3.1) and the fact that $\partial_{\mathbf{n}}(u \circ cp) = 0$ on $\partial\Omega_\delta$. \square

We are now ready to go discrete. In order to measure the denseness of a data set in a domain, say $Z \subset \Omega$, the mesh norm and the separation distance are defined as

$$h_{Z,\Omega} := \sup_{\zeta \in \Omega} \min_{z \in Z} \|z - \zeta\|_{\ell_2(\mathbb{R}^d)} \quad \text{and} \quad q_{Z,\Omega} := \frac{1}{2} \min_{\substack{z_i, z_j \in Z \\ z_i \neq z_j}} \|z_i - z_j\|_{\ell_2(\mathbb{R}^d)},$$

respectively, and the quantity $h_{Z,\Omega}/q_{Z,\Omega} =: \rho_{Z,\Omega}$ is commonly referred as the *mesh ratio* of Z . Let $d_{\mathcal{S}} : \mathcal{S} \times \mathcal{S} \rightarrow \mathbb{R}$ be the shortest distance function on \mathcal{S} . Then we also can measure these quantities on \mathcal{S} for $X \subset \mathcal{S}$ similarly by

$$h_{X,\mathcal{S}} := \sup_{\xi \in \mathcal{S}} \min_{x \in X} d_{\mathcal{S}}(x, \xi) \quad \text{and} \quad q_{X,\mathcal{S}} := \frac{1}{2} \min_{\substack{x_i, x_j \in X \\ x_i \neq x_j}} d_{\mathcal{S}}(x_i, x_j).$$

We now follow the general framework in [30] and proceed to combine some sampling and inverse inequalities in order to yield a stability result. Since we want methods that only collocate on \mathcal{S} , any available domain-type sampling [1, 2, 26] and inverse inequalities [9, 16, 17] must be used with care. First, we prove a hybrid-type sampling inequality, which aims to bound continuous norms by a discrete one defined on a set of points $X \subset \Omega$ by

$$\|w\|_{\ell^2(X)} = \left(\sum_{x_i \in X} |w(x_i)|^2 \right)^{\frac{1}{2}} \quad \text{for any } w \in \mathcal{C}(\Omega),$$

which yields strong-form collocation in our numerical formulation eventually.

THEOREM 3.3 (Sampling inequality). *Let $k \geq 2$. Suppose \mathcal{S} is of class \mathcal{C}^{m+1} for some $m \geq k + 1/2$ and $m > d/2$, and the narrow-band domain $\Omega_\delta \subset \Sigma$ has a sufficiently small δ so that Lemma 3.1 holds. Suppose further that the operators $\mathcal{L}_\mathcal{S} : \mathcal{H}^m(\mathcal{S}) \rightarrow \mathcal{H}^{m-2}(\mathcal{S})$ in (2.3) has bounded coefficients belonging to $W_\infty^m(\mathcal{S})$. Let $X \subset \mathcal{S}$ be any discrete set with sufficiently small fill distance $h_X \leq \delta$. Then there exists a constant C depending only on \mathcal{S} and $\mathcal{L}_\mathcal{S}$ such that*

$$\|\mathcal{L}_E(u \circ \text{cp})\|_{\mathcal{H}^{k-2}(\Omega_\delta)} \leq C\delta^{1/2} \left(h_X^{m-k-1/2} \|u\|_{\mathcal{H}^{m-1/2}(\mathcal{S})} + h_X^{d/2-k+3/2} \|\mathcal{L}_\mathcal{S}u\|_{\ell^2(X)} \right),$$

holds for all $u \in \mathcal{H}^m(\mathcal{S})$.

Proof. The idea of the proof is to extend $X \subset \mathcal{S}$ to a larger set in Ω_δ with controllable density and apply a domain type sampling inequality. Consider the extension

$$\widehat{X} = \{\boldsymbol{\xi} \in \Omega_\delta : \boldsymbol{\xi} = \mathbf{x} + k \cdot h_X \hat{\mathbf{n}}(\mathbf{x}), \mathbf{x} \in X, k \in \mathbb{Z}\}. \quad (3.5)$$

For sufficiently dense X , we can show by using (3.3) that $h_{\widehat{X}, \Omega_\delta} \leq c_S h_X$ for some constant $c_S \geq 1$ that does not depend on X ; see [12, Thm.6] for the details of the proof. Applying the sampling inequality in [2, Thm.3.1] to $\mathcal{L}_E(u \circ \text{cp}) \in \mathcal{H}^{m-5/2}(\Omega_\delta)$ on \widehat{X} yields

$$\begin{aligned} & \|\mathcal{L}_E(u \circ \text{cp})\|_{\mathcal{H}^{k-2}(\Omega_\delta)} \\ & \leq C_\Sigma \left(h_{\widehat{X}}^{m-k-1/2} \|\mathcal{L}_E(u \circ \text{cp})\|_{\mathcal{H}^{m-5/2}(\Omega_\delta)} + h_{\widehat{X}}^{d/2-k+2} \|\mathcal{L}_E(u \circ \text{cp})\|_{\ell^2(\widehat{X})} \right). \end{aligned}$$

In the original theorem, the generic constant in the sampling inequality depends on Ω_δ that can be further bounded by some constant C_Σ , or simply by C_S . We know that \mathcal{L}_E is a bounded operator because of $\mathcal{L}_\mathcal{S}$. By the results in [14] and Lemma 3.1, we have

$$\|\mathcal{L}_E(u \circ \text{cp})\|_{\mathcal{H}^{m-5/2}(\Omega_\delta)} \leq C_{\Omega_\delta, \mathcal{L}_E} \|u \circ \text{cp}\|_{\mathcal{H}^{m-1/2}(\Omega_\delta)} \leq C'_{\mathcal{S}, \mathcal{L}_E} \delta^{1/2} \|u\|_{\mathcal{H}^{m-1/2}(\mathcal{S})}.$$

In the first inequality, the constant $C_{\Omega_\delta, \mathcal{L}_E}$ is the supremum of the coefficients of \mathcal{L}_E and its derivatives over the domain Ω_δ and hence bounded by some $C_{\Sigma, \mathcal{L}_\mathcal{S}} = C_{\mathcal{S}, \mathcal{L}_\mathcal{S}}$. We are left to handle the discrete \widehat{X} -norm in

$$\begin{aligned} & \|\mathcal{L}_E(u \circ \text{cp})\|_{\mathcal{H}^{k-2}(\Omega_\delta)} \\ & \leq C_{\mathcal{S}, \mathcal{L}_\mathcal{S}} \left(\delta^{1/2} h_X^{m-k-1/2} \|u\|_{\mathcal{H}^{m-1/2}(\mathcal{S})} + h_X^{d/2-k+2} \|\mathcal{L}_E(u \circ \text{cp})\|_{\ell^2(\widehat{X})} \right). \end{aligned}$$

Using Taylor expansions about the corresponding closest points on \mathcal{S} along the normal direction and the constant-along-normal property of $\mathcal{L}_E(u \circ \text{cp})$, we can see that there are $2\lfloor \delta/h_{X, \mathcal{S}} \rfloor$ copies of exact data on different parallel surfaces besides of the desired $\ell^2(X)$ norm. Thus, we get

$$\|\mathcal{L}_E(u \circ \text{cp})\|_{\ell^2(\widehat{X})} \leq (1 + 2\lfloor \delta/h_X \rfloor)^{1/2} \|\mathcal{L}_E(u \circ \text{cp})\|_{\ell^2(X)}.$$

We obtain the desired sampling inequality by the fact that the sampling constant $C_{\mathcal{L}_E}$ depends only on $\mathcal{L}_\mathcal{S}$ and Σ . By requiring $h_X \leq \delta$, we have $1 + 2\lfloor \delta/h_X \rfloor \leq C\delta/h_X$. \square

Up to this point, we are still in full Sobolev spaces. Now, we need an appropriate inverse inequality to bound the $\mathcal{H}^3(\mathcal{S})$ norm in Theorem 3.3 by some weaker norms on

\mathcal{S} . Such inequalities are available for functions in the native space of certain kernels. More specifically, we consider translation-invariant symmetric positive definite kernels $\Phi_m : \mathbb{R}^d \times \mathbb{R}^d \rightarrow \mathbb{R}$ with smoothness m that satisfy

$$c_{\Phi_m}(1 + \|\omega\|_2^2)^{-m} \leq \widehat{\Phi_m}(\omega) \leq C_{\Phi_m}(1 + \|\omega\|_2^2)^{-m} \quad \text{for all } \omega \in \mathbb{R}^d, \quad (3.6)$$

for some constants $0 < c_{\Phi_m} \leq C_{\Phi_m}$. This includes the standard Whittle-Matérn-Sobolev kernels, that are defined via the Bessel functions of the second kind in the form of $\Phi_m(x) := \|x\|_2^{m-\frac{d}{2}} \mathcal{K}_{m-\frac{d}{2}}(\|x\|_2)$, and the compactly supported piecewise polynomial Wendland functions [36]. We denote the associated reproducing kernel Hilbert space, a.k.a. the native space, of these kernels by $\mathcal{N}_{\Omega, \Phi_m}$. For any $m > d/2$, the native space $\mathcal{N}_{\Omega, \Phi_m}$ is norm-equivalent to $\mathcal{H}^m(\Omega)$ provided Ω satisfies some standard smoothness assumptions [6, 37].

Let $Z = \{z_1, \dots, z_{n_Z}\}$ be a discrete set of trial centers in some domain Ω . We define the corresponding finite-dimensional trial space by

$$\mathcal{U}_{Z, \Omega, \Phi_m} := \text{span}\{\Phi_m(\cdot - z_j) : z_j \in Z\} \subset \mathcal{N}_{\Omega, \Phi_m}.$$

Functions in the trial space have many special features. We now provide an inverse inequality that is suitable to our context.

THEOREM 3.4 (Inverse inequality). *Let $k > d/2$. Suppose \mathcal{S} is of class \mathcal{C}^{m+1} for some $m \geq k$ and the narrow-band domain $\Omega_\delta \subset \Sigma$ has a sufficiently small δ so that Lemma 3.1 holds. Suppose a kernel $\Phi_m : \mathbb{R}^d \times \mathbb{R}^d \rightarrow \mathbb{R}$ satisfying (3.6) is given. Let $Z \subset \Omega_\delta$ be any set of sufficiently dense trial centers. Then there exists a constant C depending only on \mathcal{S} , Φ_m , ρ_Z and k such that the inequality*

$$\|u\|_{\mathcal{H}^{m-1/2}(\mathcal{S})} \leq C\delta^{-1/2}h_Z^{-m+k} \left(\|u\|_{\mathcal{H}^k(\mathcal{S})} + h_Z^{-k+d/2} \|u - u|_{\mathcal{S}} \circ \text{cp}\|_{\ell^2(Z)} \right)$$

holds for all trial functions $u \in \mathcal{U}_{Z, \Omega_\delta, \Phi_m}$.

Proof. Let $I_Z u_{\text{cp}} := I_{Z, \Omega_\delta, \Phi_m}(u|_{\mathcal{S}} \circ \text{cp})$ denote the unique interpolant of $u|_{\mathcal{S}} \circ \text{cp}$ on Z from $\mathcal{U}_{Z, \Omega_\delta, \Phi_m}$. Since $u|_{\mathcal{S}} \circ \text{cp}$ is Z -dependent, we shall not rely on any convergence result regarding $I_Z u_{\text{cp}} \rightarrow u|_{\mathcal{S}} \circ \text{cp}$ in this proof. Using a trace theorem with an explicit δ -dependent constant, which can be extracted easily from [10, 15],

$$\begin{aligned} \|u\|_{\mathcal{H}^{m-1/2}(\mathcal{S})} &\leq C_S \delta^{-1/2} \|u\|_{\mathcal{H}^m(\Omega_\delta)} \\ &\leq C_S \delta^{-1/2} \left(\|I_Z u_{\text{cp}}\|_{\mathcal{H}^m(\Omega_\delta)} + \|u - I_Z u_{\text{cp}}\|_{\mathcal{H}^m(\Omega_\delta)} \right). \end{aligned}$$

For any $k > d/2$ and $m \geq k$, we can invoke the inverse inequality [9, Lem.3.2] within the trial space $\mathcal{U}_{Z, \Omega_\delta, \Phi_m}$ to obtain

$$\|I_Z u_{\text{cp}}\|_{\mathcal{H}^m(\Omega_\delta)} \leq C_{\mathcal{S}, \Phi_m, k} h_Z^{-m+k} \|I_Z u_{\text{cp}}\|_{\mathcal{H}^k(\Omega_\delta)}. \quad (3.7)$$

For any ρ_Z -uniform $Z \subset \Omega$, $m > d/2$ and $m \geq k$, by [28, Cor.4.3], the interpolation map $I_Z := I_{Z, \Omega_\delta, \Phi_m} : \mathcal{H}^k(\Omega_\delta) \rightarrow \mathcal{H}^m(\Omega_\delta)$ with $k < m$ and kernel Φ_m is bounded uniformly in Z . Hence, by Lemma 3.1, we can further bound (3.7) from the above by

$$\begin{aligned} \|I_Z u_{\text{cp}}\|_{\mathcal{H}^m(\Omega_\delta)} &\leq C_{\Omega_\delta, \Phi_m, k, \rho_Z} h_Z^{-m+k} \|u|_{\mathcal{S}} \circ \text{cp}\|_{\mathcal{H}^k(\Omega_\delta)} \\ &\leq C_{\Omega_\delta, \Phi_m, k, \rho_Z} \delta^{1/2} h_Z^{-m+k} \|u\|_{\mathcal{H}^k(\mathcal{S})}. \end{aligned}$$

After inspecting the proofs (Cor.3.5 in particular), we see that the constant here depends on the norm of a Sobolev extension map $\mathcal{E}_{\Omega_\delta, k} : \mathcal{H}^k(\Omega_\delta) \rightarrow \mathcal{H}^k(\mathbb{R}^d)$ and hence $C_{\Omega_\delta, \Phi_m, k, \rho_Z} \leq \delta^{-1/2} C_{\mathcal{S}, \Phi_m, k, \rho_Z}$.

Since $u - I_Z u_{\text{cp}} \in \mathcal{U}_{Z, \Omega_\delta, \Phi_m}$, the magnitude of $\|u - I_Z u_{\text{cp}}\|_{\mathcal{H}^m(\Omega_\delta)}$ is completely determined by the function values of $u - I_Z u_{\text{cp}}$ at Z . To prove this, we rely on the norm equivalency of $\mathcal{H}^m(\mathbb{R}^d)$ and $\mathcal{N}_{\Phi_m}(\mathbb{R}^d)$, and the eigenvalue estimate of the kernel matrix $\Phi_m(Z, Z)$ in [28] to obtain

$$\begin{aligned} \|u - I_Z u_{\text{cp}}\|_{\mathcal{H}^m(\Omega_\delta)} &\leq \|u - I_Z u_{\text{cp}}\|_{\mathcal{H}^m(\mathbb{R}^d)} \\ &\leq C_{\Phi_m} \|u - I_Z u_{\text{cp}}\|_{\mathcal{N}_{\Phi_m}(\mathbb{R}^d)} \\ &= C_{\Phi_m} \|u - I_Z u_{\text{cp}}\|_{\mathcal{N}_{\Phi_m}(\Omega_\delta)} \\ &\leq C_{\Phi_m} \|\Phi_m(Z, Z)^{-1}\|_2^{1/2} \|u - I_Z u_{\text{cp}}\|_{\ell^2(Z)} \\ &\leq C_{\Phi_m} q_Z^{-m+d/2} \|u - I_Z u_{\text{cp}}\|_{\ell^2(Z)} \end{aligned}$$

for any $u \in \mathcal{U}_{Z, \Omega_\delta, \Phi_m}$. Noting that the functions $I_Z u_{\text{cp}} = I_Z(u|_{\mathcal{S}} \circ \text{cp})$ and $u|_{\mathcal{S}} \circ \text{cp}$ coincide at node Z completes the proof. \square

We now have all the necessary components to derive an embedding PDE and the associated stability estimate. Let $X \subset \mathcal{S}$ be any discrete set of sufficiently dense collocation points. Using Theorem 3.2 and Theorem 3.3, we immediately obtain

$$\begin{aligned} \|u\|_{\mathcal{H}^k(\mathcal{S})} &\leq C_S \delta^{-1/2} \|\mathcal{L}_E(u \circ \text{cp})\|_{\mathcal{H}^{k-2}(\Omega_\delta)} \\ &\leq C_{\mathcal{S}, \mathcal{L}_S} \left(h_X^{m-k-1/2} \|u\|_{\mathcal{H}^{m-1/2}(\mathcal{S})} + h_X^{d/2-k+3/2} \|\mathcal{L}_S u\|_{\ell^2(X)} \right). \end{aligned}$$

By employing a kernel Φ_m with higher order of smoothness $m > k + 1/2 + d/2$ and defining its trial space using a set of distinct trial centers $Z \subset \Omega_\delta$, we ensure that the restrictions of all trial functions are smooth enough, i.e., $u|_{\mathcal{S}} \in \mathcal{H}^m(\mathcal{S})$ for all $u \in \mathcal{U}_{Z, \Omega_\delta, \Phi_m}$, for the theories to be applied. Under a sufficient condition

$$h_X^{m-d/2-k+\epsilon} \sim \delta^{1/2} h_Z^{m-d/2}, \quad \text{for any } \epsilon > 0 \quad (3.8)$$

which ensures

$$(C_{\mathcal{S}, \mathcal{L}_S} h_X^{m-k-1/2}) (C_{\mathcal{S}, \Phi_m, k, \rho_Z} \delta^{-1/2} h_Z^{-m+k}) h_Z^{-k+d/2} h_X^{-(d/2-k+3/2)} = \mathcal{O}(h_X^\epsilon),$$

Theorem 3.4 suggests that

$$\|u\|_{\mathcal{H}^k(\mathcal{S})} \leq C_{\mathcal{S}, \mathcal{L}_S, \Phi_m, k, \rho_Z} h_X^{d/2-k+3/2} \left(\|\mathcal{L}_S u\|_{\ell^2(X)} + h_X^\epsilon \|u - u|_{\mathcal{S}} \circ \text{cp}\|_{\ell^2(Z)} \right).$$

At last, we obtain the following stability estimate within trial spaces.

THEOREM 3.5 (Stability). *Let $k \geq 2$ and $k > d/2$. Suppose the assumptions in Theorems 3.2, 3.3 and 3.4 hold for some $m > k + 1/2 + d/2$. Let $X \subset \mathcal{S}$ be any discrete set with sufficiently small fill distance $h_X \leq \delta$ so that condition (3.8) holds for some $\epsilon > 0$. Then there exists a constant C depending only on \mathcal{S} , Φ_m , \mathcal{L}_S , k and ρ_Z such that the inequality*

$$\|u\|_{\mathcal{H}^k(\mathcal{S})} \leq C h_X^{d/2-k+3/2} \left(\|\mathcal{L}_S u\|_{\ell^2(X)} + h_X^\epsilon \|u - u|_{\mathcal{S}} \circ \text{cp}\|_{\ell^2(Z)} \right),$$

holds for all trial functions $u \in \mathcal{U}_{Z, \Omega_\delta, \Phi_m}$.

4. Embedded Kansa methods and convergence estimate. After picking a value of δ , the stability estimate in Theorem 3.5 immediately gives rise to a strong-form collocation method. It is clear that δ cannot be arbitrarily small; due to the radial shape of the trial basis functions, we must have $Z \cap (\mathbb{R} \setminus \mathcal{S}) \neq \emptyset$ in order to have the embedding conditions in Theorem 2.1 approximately satisfied. That is, $\delta \approx h_{Z, \Omega_\delta}$ is the most computationally efficient selection, which agrees perfectly with the setup of the orthogonal gradients method [29]. Moreover, Theorem 3.5 allows Z to be scattered in Ω_δ , which helps maximizing q_Z .

THEOREM 4.1 (Convergence). *Let $k \geq 2$ and $k > d/2$. Suppose $u_{\mathcal{S}}^* \in \mathcal{H}^m(\mathcal{S})$ with Sobolev smoothness order $m > k + d/2 + 1/2$ is the solution of the surface PDE (1.1). Suppose all the other assumptions in Theorem 3.5 hold. Let $u_{X,Z} \in \mathcal{U}_{Z, \Omega_\delta, \Phi_m}$ be the least-squares Kansa solution defined by*

$$\arg \inf_{u \in \mathcal{U}_{Z, \Omega_\delta, \Phi_m}} \left(\underbrace{\|\mathcal{L}_E u - f\|_{\ell^2(X)}^2}_{\text{PDE collocations}} + \underbrace{\|\partial_{\hat{\mathbf{n}}} u\|_{\ell^2(X)}^2 + \|\partial_{\hat{\mathbf{n}}}^{(2)} u\|_{\ell^2(X)}^2}_{\text{Embedding conditions}} + h_X^\epsilon \underbrace{\|u - u_{\mathcal{S}} \circ \text{cp}\|_{\ell^2(Z)}^2}_{\text{Stability conditions}} \right).$$

Then the estimate

$$\begin{aligned} & \|u_{X,Z} - u_{\mathcal{S}}^*\|_{\mathcal{H}^k(\mathcal{S})} \\ & \leq C \left(\underbrace{h_Z^{m-k-1/2-d/2}}_{\text{Interpolation error}} + \underbrace{\delta^{1/2} h_X^{2-k} h_Z^{m-2-d/2}}_{\text{PDE error}} + \underbrace{\delta h_X^{d/2-k+3/2+\epsilon} h_Z^{m-d}}_{\text{Stability error}} \right) \|u_{\mathcal{S}}^*\|_{\mathcal{H}^m(\mathcal{S})} \end{aligned}$$

holds for some constant C depending only on \mathcal{S} , Φ_m , $\mathcal{L}_{\mathcal{S}}$, k , ρ_Z and ρ_X . With higher smoothness order $m > k + d/2 + 3/2$, we have an improved error bound for interpolation and

$$\begin{aligned} & \|u_{X,Z} - u_{\mathcal{S}}^*\|_{\mathcal{H}^k(\mathcal{S})} \\ & \leq C' \left(h_Z^{m-k-1/2} + \delta^{1/2} h_X^{2-k} h_Z^{m-2-d/2} + \delta h_X^{d/2-k+3/2+\epsilon} h_Z^{m-d} \right) \|u_{\mathcal{S}}^*\|_{\mathcal{H}^m(\mathcal{S})} \end{aligned}$$

holds for another constant C' with the same dependencies.

Proof. The convergence estimate can be obtained by following the general framework in [9]. Note that the stability estimate in Theorem 3.5 only holds for functions in the trial space $\mathcal{U}_{Z, \Omega_\delta, \Phi_m}$. To obtain an error estimate, see [37, Thm.11.9] and [11, Sec.15.1.2], we need the following manipulations:

$$\|u_{X,Z} - u_{\mathcal{S}}^*\|_{\mathcal{H}^k(\mathcal{S})} \leq \|u_{X,Z} - I_Z u_{\text{cp}}^*\|_{\mathcal{H}^k(\mathcal{S})} + \|I_Z u_{\text{cp}}^* - u_{\mathcal{S}}^*\|_{\mathcal{H}^k(\mathcal{S})}, \quad (4.1)$$

where $I_Z u_{\text{cp}}^* = I_{Z, \Omega_\delta, \Phi_m}(u_{\mathcal{S}}^* \circ \text{cp})$ is the unique interpolant of $u_{\text{cp}}^* := u_{\mathcal{S}}^* \circ \text{cp}$ on Z from the trial space $\mathcal{U}_{Z, \Omega_\delta, \Phi_m}$. For $m > k + 1/2 + d/2$, applying meshfree convergence estimates and Lemma 3.1 yields the ‘‘interpolation error’’

$$\begin{aligned} \|I_Z u_{\text{cp}}^* - u_{\mathcal{S}}^*\|_{\mathcal{H}^k(\mathcal{S})} &= \|I_Z u_{\text{cp}}^* - u_{\text{cp}}^*\|_{\mathcal{H}^k(\mathcal{S})} \\ &\leq C_{\mathcal{S}} \delta^{-1/2} \|I_Z u_{\text{cp}}^* - u_{\text{cp}}^*\|_{\mathcal{H}^{k+1/2}(\Omega_\delta)} \\ &\leq C_{\mathcal{S}, \Sigma, \Phi_m} \delta^{-1/2} h_Z^{m-k-1/2-d/2} \|u_{\text{cp}}^*\|_{\mathcal{H}^m(\Omega_\delta)} \\ &\leq C_{\mathcal{S}, \Sigma, \Phi_m} h_Z^{m-k-1/2-d/2} \|u_{\mathcal{S}}^*\|_{\mathcal{H}^m(\mathcal{S})}. \end{aligned}$$

For larger values of $m > k + 3/2 + d/2$, one can use [27, Prop.3.3] to achieve higher convergence rates of $m - k - 1/2$.

If we define a functional by

$$J^2(u) := \|\mathcal{L}_E u\|_{\ell^2(X)}^2 + \|\partial_{\hat{\mathbf{n}}} u\|_{\ell^2(X)}^2 + \|\partial_{\hat{\mathbf{n}}}^{(2)} u\|_{\ell^2(X)}^2 + h_X^\epsilon \|u - u|_{\mathcal{S}} \circ \text{cp}\|_{\ell^2(Z)}^2,$$

then, by definition, the Kansa solution $u_{X,Z}$ minimizes $J^2(u_{\text{cp}}^* - u)$ over the trial space $\mathcal{U}_{Z,\Omega_\delta,\Phi_m}$. Therefore, we get an overestimate if $u_{X,Z}$ is replaced by any other function in the trial space; in particular, we use the interpolant $I_Z u_{\text{cp}}^* \circ \text{cp}$ as a comparison function. By Theorem 3.5 and Corollary 2.2, the minimization property of $u_{X,Z}$ suggests that

$$\begin{aligned} \|u_{X,Z} - I_Z u_{\text{cp}}^*\|_{\mathcal{H}^k(\mathcal{S})} &\leq C_{\mathcal{S},\Phi_m,\mathcal{L}_S,k,\rho_Z} h_X^{d/2-k+3/2} \left(J(u_{\text{cp}}^* - u_{X,Z}) + J(u_{\text{cp}}^* - I_Z u_{\text{cp}}^*) \right) \\ &\leq 2C_{\mathcal{S},\Phi_m,\mathcal{L}_S,k,\rho_Z} h_X^{d/2-k+3/2} J(u_{\text{cp}}^* - I_Z u_{\text{cp}}^*). \end{aligned} \quad (4.2)$$

Firstly, we bound the PDE residual and embedding errors in $J(u_{\text{cp}}^* - I_Z u_{\text{cp}}^*)$ with similar technique. For any $m > 2 + d/2$, we can estimate the ‘‘PDE error’’ as follows:

$$\begin{aligned} \|\mathcal{L}_E(I_Z u_{\text{cp}}^* - u_{\text{cp}}^*)\|_{\ell^2(X)}^2 + \|\partial_{\hat{\mathbf{n}}}(I_Z u_{\text{cp}}^* - u_{\text{cp}}^*)\|_{\ell^2(X)}^2 + \|\partial_{\hat{\mathbf{n}}}^{(2)}(I_Z u_{\text{cp}}^* - u_{\text{cp}}^*)\|_{\ell^2(X)}^2 \\ \leq C_{\mathcal{S},\mathcal{L}_S} \sum_{|\alpha| \leq 2} \|D^\alpha(I_Z u_{\text{cp}}^* - u_{\text{cp}}^*)\|_{\ell^2(X)}^2 \\ \leq C'_{\mathcal{S},\mathcal{L}_S} n_X \max_{|\alpha| \leq 2} \|D^\alpha(I_Z u_{\text{cp}}^* - u_{\text{cp}}^*)\|_{L^\infty(\Omega_\delta)}^2 \\ \leq C'_{\mathcal{S},\mathcal{L}_S} (C_S q_X^{-(d-1)}) C_{\Sigma,\Phi_m} h_Z^{2m-4-d} \|u_{\text{cp}}^*\|_{\mathcal{H}^m(\Omega_\delta)}^2 \\ \leq C_{\mathcal{S},\Phi_m,\mathcal{L}_S,\rho_X} \delta h_X^{-d+1} h_Z^{2m-4-d} \|u_{\text{cp}}^*\|_{\mathcal{H}^m(\mathcal{S})}^2. \end{aligned} \quad (4.3)$$

For any $z \in Z$, we have

$$(I_Z u_{\text{cp}}^*)(z) = u_{\text{cp}}^*(z) = u_{\mathcal{S}}^*(\text{cp}(z)) \quad \text{and} \quad ((I_Z u_{\text{cp}}^*)|_{\mathcal{S}} \circ \text{cp})(z) = (I_Z u_{\text{cp}}^*)(\text{cp}(z)).$$

Thus, for $m > d/2$, the ‘‘stability error’’ in $J(u_{\text{cp}}^* - I_Z u_{\text{cp}}^*)$ can be bounded by

$$\begin{aligned} \|(I_Z u_{\text{cp}}^* - u_{\text{cp}}^*) - (I_Z u_{\text{cp}}^* - u_{\text{cp}}^*)|_{\mathcal{S}} \circ \text{cp}\|_{\ell^2(Z)}^2 &= \|I_Z u_{\text{cp}}^* - (I_Z u_{\text{cp}}^*)|_{\mathcal{S}} \circ \text{cp}\|_{\ell^2(Z)}^2 \\ &\leq n_Z \|u_{\mathcal{S}}^* - I_Z u_{\text{cp}}^*\|_{L^\infty(\mathcal{S})}^2 \leq n_Z \|u_{\text{cp}}^* - I_Z u_{\text{cp}}^*\|_{L^\infty(\Omega_\delta)}^2 \\ &\leq (C_S \delta q_Z^{-d}) h_Z^{2m-d} \|u_{\text{cp}}^*\|_{\mathcal{H}^m(\Omega_\delta)}^2 \leq C_{\mathcal{S},\rho_Z} \delta^2 h_Z^{2m-2d} \|u_{\mathcal{S}}^*\|_{\mathcal{H}^m(\mathcal{S})}^2. \end{aligned} \quad (4.4)$$

Putting (4.3) and (4.4) into (4.2) yields the asserted estimate. \square

It is worth pointing out that ‘‘PDE+Embedding conditions¹’’ and ‘‘PDE+Stability conditions’’ were considered as two different numerical recipes in [29]. The numerical demonstrations there show that ‘‘PDE+Embedding conditions’’ yields better performance. Readers can see that the embedding and stability conditions have their own roles to play in our analysis. Both conditions are necessary to ensure high order convergence.

Before presenting any numerical result, let us first go over some implementation details. Our theories allow more general setting than that of the orthogonal gradients method. For trial centers $Z \subset \Omega_\delta$, one needs not keeping all the off-surface centers in the orthogonal direction of some $z_i \in Z \cap \mathcal{S}$. Since the end user has complete

¹Embedding conditions in [29] are $n \cdot \nabla u = 0$ and $(\hat{\mathbf{n}} \cdot \nabla)(\hat{\mathbf{n}} \cdot \nabla)u = 0$ instead of our Theorem 2.1.

control over the distribution of Z , it makes sense to place quasi-uniform trial centers on \mathcal{S} and then extend (either orthogonally or by other means) them out-of-surface by distance $h_{Z,\mathcal{S}}$ to form a quasi-uniform set $Z \subset \Omega_\delta$. Collocation points in X should be sufficiently dense to ensure stability, see (3.8) for a sufficient condition, and ideally quasi-uniform, can be placed on \mathcal{S} . By comparing to the optimal result in the domain analogy [9], which only requires linear ratio of oversampling $h_X \leq Ch_Z$, the sufficient condition (3.8) is unlikely to be a necessary one.

Firstly, we consider the ‘‘PDE collocations’’ part. Although \mathcal{L}_E is defined by the cp-extension of $\mathcal{L}_\mathcal{S}$, the discrete norm $\|\mathcal{L}_E u\|_{\ell^2(X)}$ does not require any information away from \mathcal{S} . When implemented, it is unnecessary to cp-extend the coefficients of $\mathcal{L}_\mathcal{S}$. Also note that there are many zeros in the stability conditions, viz., $\|u - u|_\mathcal{S} \circ \text{cp}\|_{\ell^2(Z)}^2 = \|u - u|_\mathcal{S} \circ \text{cp}\|_{\ell^2(Z \setminus \mathcal{S})}^2$. Thus, the overdetermined linear system in Theorem 4.1 can be written in matrix form as

$$\begin{pmatrix} \mathcal{L}_E \Phi_m(X, Z) \\ \partial_{\hat{\mathbf{n}}} \Phi_m(X, Z) \\ \partial_{\hat{\mathbf{n}}}^{(2)} \Phi_m(X, Z) \\ \Phi_m(Z \setminus \mathcal{S}, Z) - \Phi_m(\text{cp}(Z \setminus \mathcal{S}), Z) \end{pmatrix} \boldsymbol{\lambda} = \begin{pmatrix} f(X) \\ \mathbf{0} \\ \mathbf{0} \\ \mathbf{0} \end{pmatrix}, \quad (4.5)$$

in which all differential operators act on the first argument of Φ_m . Once we obtain the least-squares solution $\boldsymbol{\lambda} = \{\lambda_i\}_{i=1}^{n_Z}$, the Kansa solution can be evaluated everywhere on \mathcal{S} by $u_{X,Z}(\cdot) = \sum_{\zeta_i \in Z} \lambda_i \Phi_m(\cdot, \zeta_i)$.

From Theorem 3.5, we can see that the ‘‘stability conditions’’ with a weight h_X^ϵ is asymptotically insignificant as $h_X \rightarrow 0$. Moreover, the corresponding ‘‘stability error’’ in Theorem 4.1 is much smaller than the others. Theoretically, the stability conditions can be approximated by the embedding conditions plus an $\mathcal{O}(\delta)$ Taylor residual error and the ‘‘PDE+Embedding conditions’’ formulation remains low-order convergent by our Theorem 3.5. Moreover, it has the smallest length scale as all the other blocks involve derivatives of the kernel. All these justifications hint that the ‘‘stability conditions’’ are numerically negligible. Our first example in Section 5 aims to identify appropriate numerical setups for practical use.

5. Numerical examples. We present three numerical examples aiming to address a few practical problems concerning the proposed kernel-based embedding method. The first example aims to identify the smoothness and necessary denseness requirements on the kernel and the set of collocation points $X \subset \mathcal{S}$ respectively. The second studies the effect when data points, Z and/or X , are not unevenly distributed and the curvature of the surface becomes large. The last shows some simulated results when the proposed method is applied to time-dependent PDEs. Among all of the numerical experiments, we use a scaled Whittle-Matérn-Sobolev kernel in the form of $\Phi_m(x) := (m\|x\|_2)^{m-\frac{d}{2}} \mathcal{K}_{m-\frac{d}{2}}(m\|x\|_2)$ in order to minimize the effect of ill-conditioning.

EXAMPLE 5.1 (Denseness and smoothness requirements). We consider overdetermined systems in the form of

$$\|\mathcal{L}_E u - f\|_{\ell^2(X)}^2 + \|\mathcal{W}_1 \partial_{\hat{\mathbf{n}}} u\|_{\ell^2(X)}^2 + \|\mathcal{W}_2 \partial_{\hat{\mathbf{n}}}^{(2)} u\|_{\ell^2(X)}^2 + \mathcal{W}_3 \|u - u|_\mathcal{S} \circ \text{cp}\|_{\ell^2(\hat{X})}^2$$

with different weightings $\mathcal{W}_1, \mathcal{W}_2 : \mathcal{S} \rightarrow \mathbb{R}$ and $\mathcal{W}_3 \in \mathbb{R}$. The linear system in (4.5) corresponds to $\mathcal{W}_1 = 1 = \mathcal{W}_2$ and $\mathcal{W}_3 = \min(1, h_X^\epsilon)$. When condition (3.8) is satisfied, we have $\mathcal{W}_3 = h_X^\epsilon$ as defined in Theorem 4.1. Using Theorem 2.1, we can reintroduce

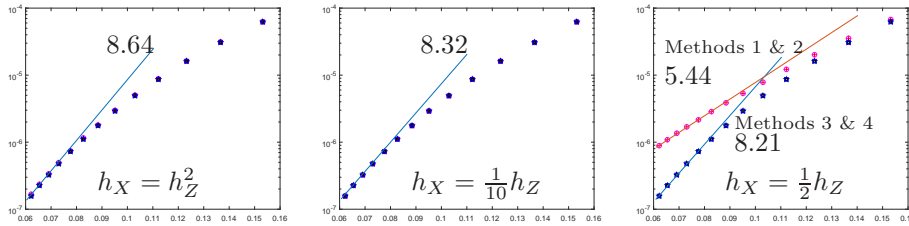


FIG. 5.1. *Example 1: The $\mathcal{H}^2(\mathcal{S})$ convergence profiles of the proposed method with different denseness of collocation points for solving a modified Helmholtz problem on the unit circle.*

the geometry of \mathcal{S} back into the linear system by setting $\mathcal{W}_1 = aH_{\mathcal{S}} - \mathbf{b} \cdot \hat{\mathbf{n}}$ and $\mathcal{W}_2 = a$ where a and \mathbf{b} are coefficients of the embedding PDE in (1.2). Furthermore, setting $\mathcal{W}_3 = 0$ drops the “embedding conditions” from the linear system. Formulations to be tested are:

Method 1: A full system with $\mathcal{W}_1 = aH_{\mathcal{S}} - \mathbf{b} \cdot \hat{\mathbf{n}}$, $\mathcal{W}_2 = a$, and $\mathcal{W}_3 = \min(1, h_X^\epsilon)$.

Method 2: A full system with $\mathcal{W}_1 = 1$, $\mathcal{W}_2 = 1$, and $\mathcal{W}_3 = \min(1, h_X^\epsilon)$.

Method 3: A reduced system with $\mathcal{W}_1 = aH_{\mathcal{S}} - \mathbf{b} \cdot \hat{\mathbf{n}}$, $\mathcal{W}_2 = a$, and $\mathcal{W}_3 = 0$.

Method 4: A reduced system with $\mathcal{W}_1 = 1$, $\mathcal{W}_2 = 1$, and $\mathcal{W}_3 = 0$.

All four formulations are applied to solve a surface modified Helmholtz equation in the unit circle and an ellipse in \mathbb{R}^2 . Trial centers $Z \cap \mathcal{S}$ are placed on the curves and orthogonally extended in- and outward to form the full set of collocation points Z as in the orthogonal gradients method [29]. Collocation points X are uniformly distributed on \mathcal{S} .

To numerically seek for a necessary denseness condition, we consider different relative fill distances $h_X = \frac{1}{2}h_Z$, $h_X = \frac{1}{10}h_Z$ and lastly, a theoretically sufficient one $h_X = h_Z^2$ with $\epsilon = 2 - 11/6$. All reported errors are in $\mathcal{H}^2(\mathcal{S})$ approximated on a dense set of evaluation points by an equivalent norm $\|(I - \Delta_{\mathcal{S}})u\|_{L^2(\mathcal{S})}$ based on the relationships in (2.4).

In Figure 5.1, the $\mathcal{H}^2(\mathcal{S})$ errors with different h_X resulting from an $m = 6$ kernel are plotted against the fill distance h_Z . When the sufficient condition is satisfied, all four methods yield the same convergence and accuracy. The same conclusion remains valid if the denseness is relaxed to $h_X = \frac{1}{10}h_Z$. If we further reduce the denseness to $h_X = \frac{1}{2}h_Z$, we can see that both convergence and accuracy of Methods 1 and 2 are affected, whereas Methods 3 and 4 remain as accurate as the previous cases. Instead of finding a proper formula of \mathcal{W}_3 to “violate” the denseness requirement in Theorem 4.1, this demonstration suggests that we can simply drop the “stability conditions” whose numerical importance is insignificant.

Next, we study the convergence rate with respect to the smoothness of the kernel. Figure 5.2 shows the $\mathcal{H}^2(\mathcal{S})$, i.e., $k = 2$, and $L^2(\mathcal{S})$ error profiles of Methods 3 and 4 for solving a modified Helmholtz equation on an ellipse with an axis ratio $a/b = 2$ and circumference 2π . It is trivial to see that the orders of convergence increase with the smoothness parameter $m > k + 1/2 + d/2$. We can also see that the added “geometry” does not help improve the accuracy of Method 3. Moreover, incrementing m by 1 results in two extra orders of convergence in $\mathcal{H}^2(\mathcal{S})$ errors. In the next example, we will explore more about this idea.

EXAMPLE 5.2 (Uniformities of data sets). Numerical evidence in Example 5.1 suggests that the economical Methods 3 and 4, which only collocates the embedding PDE and our proposed embedding conditions, performs as well as the theoretically

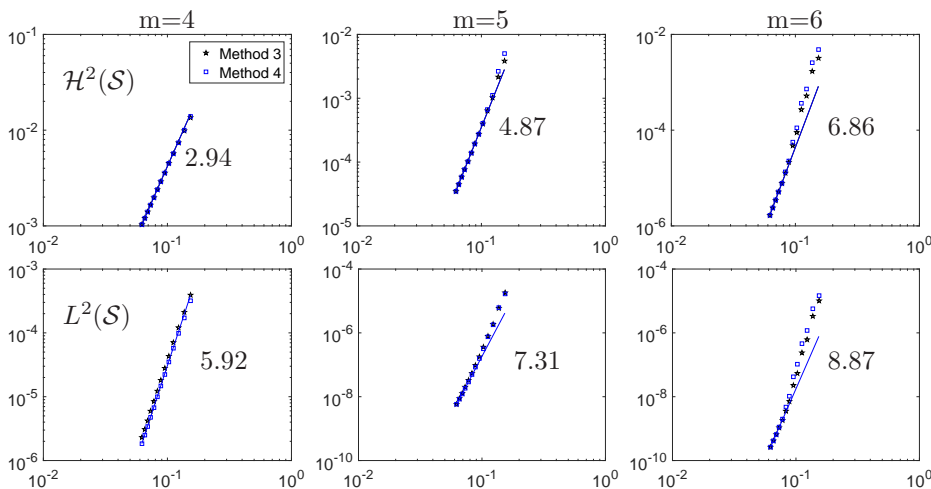


FIG. 5.2. Example 1: Convergence profiles for various different smoothness m of the reduced systems (Methods 3 and 4) on an ellipse with axis ratio $a/b = 2$.

convergent Methods 1 and 2.

We continue to study the importance of having surface geometry in the formulation (i.e., \mathcal{W}_1 and \mathcal{W}_2) by solving the modified Helmholtz equation in Example 5.1 on two ellipses with different axis ratio $a/b = 3$ and $= 5$, see Figure 5.3. The problems are solved by Methods 3 and 4 with $h_Z = \frac{1}{10}h_X$. To show that the proposed method is easy to apply for most users, we simply generate the sets X and Z by using regular data from the parameter space of and unevenly distributed data points on \mathcal{S} .

For comparison, results obtained by the projection method in [13] are also included. Note that data points used there are relatively uniform and, in our test problems, we can see the solutions of the projection method oscillate (around the antipodal points along the major axis where the data points density is high). Such numerical instability is typical in high-order meshfree interpolation. In contrast, our proposed least-squares formulation is more easygoing in nonuniform data points. We can see that orders of convergence of both Methods 3 and 4 (with $m = 6$) are similar. Obviously, Method 3, which makes use of the geometry of \mathcal{S} , should better capture the embedding PDE and it is of no surprise to see that its $\mathcal{H}^2(\mathcal{S})$ error is smaller. However, the situation is reversed if we consider their $L^2(\mathcal{S})$ errors. We can easily see the error in the solution of Method 3 in the case of $a/b = 5$. Method 4, which is the simplest formulation among the tested ones, indeed is the most reliable one. Note that the tested range of h_Z is quite small here. With large eccentricity, the estimated $\mathcal{H}^2(\mathcal{S})$ -convergence rate of Method 4 is about 3.54, which agrees nicely with the predicted $m - k - 1/2 = 3.5$ order by our theories. This suggests that the higher-than-predicted orders of convergence of meshfree method reported in literature only hold on some surfaces.

Next, we consider a modified Helmholtz on an ellipsoid² or a torus³ in \mathbb{R}^3 . In Figure 5.4, we show the error distributions for the numerical approximation obtained by $m = 6$, and the convergence profiles of Method 4 and the projection methods with various smoothness parameter m . The observations made here are similar to above.

² $x^2 + (y/1.5)^2 + (z/0.5391)^2$.

³ $(1 - \sqrt{x^2 + y^2})^2 + z^2 = 1/9$.

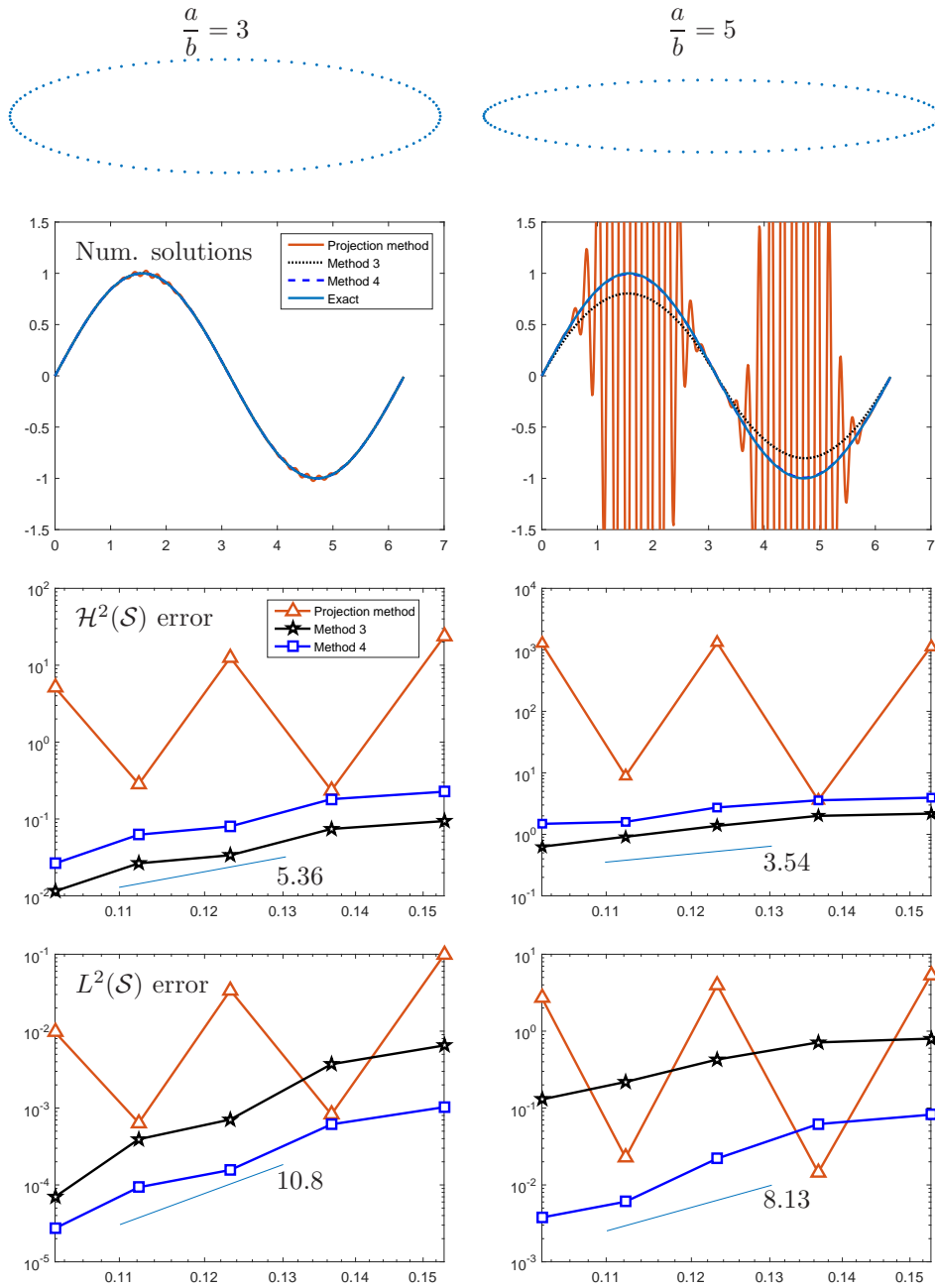


FIG. 5.3. Example 2: Numerical results of the proposed method with $m = 6$ and the projection method in [13] for solving a modified Helmholtz equation on ellipses with different axis ratio $\frac{a}{b}$.

We can see that large absolute error accumulates near regions with large mean curvature of the ellipsoid despite the high density of data points, but around the outer surface of the Torus where data points are coarser. Convergence behaviours in $L^2(\mathcal{S})$ are also provided for different kernel smoothness m . In terms of convergence, we

can see that, for each m , the projection method and Method 4 have similar convergence rates. As for accuracy, it is really up to the surface and its curvature; our method is more accurate on the ellipsoid whereas the projection method yields better approximations on the torus.

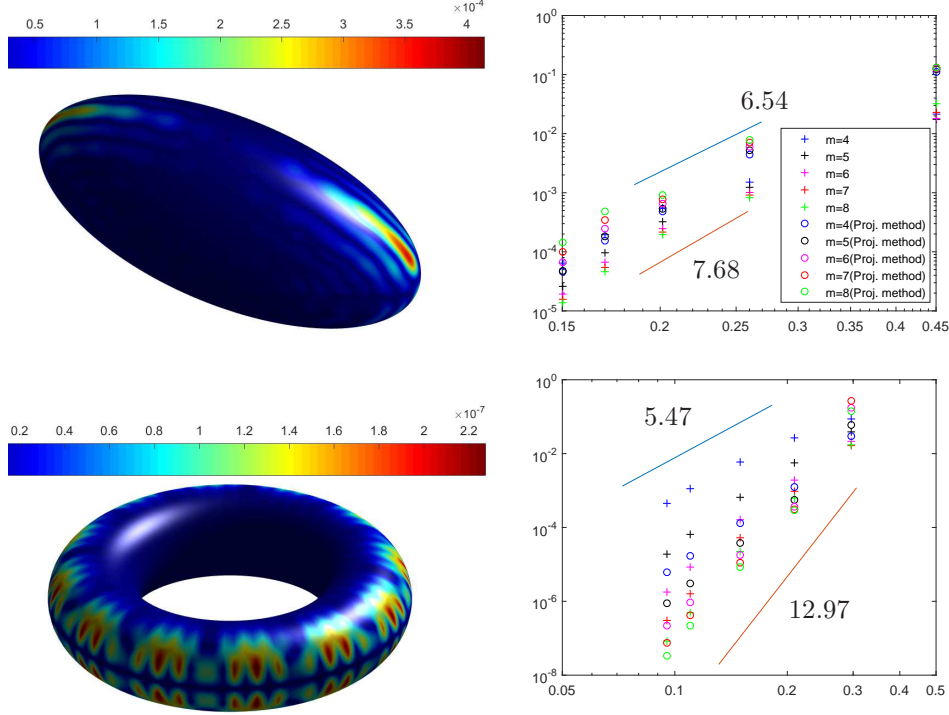


FIG. 5.4. Example 2: Absolute error plot and convergence plot for torus and ellipsoid.

EXAMPLE 5.3 (Reaction diffusion equations). The previous examples focus on solving second order elliptic equations. It would be interesting to apply the proposed method to solve time-dependent PDEs on surface. This example concerns about numerical simulations of reaction diffusion equation for pattern formations on surfaces. Consider the following system of equations [5, 35] for the *Turing spot* and *stripe patterns*:

$$\frac{\partial u}{\partial t} = \delta_u \Delta_{\mathcal{S}} u + f_u(u, v) \quad \text{and} \quad \frac{\partial v}{\partial t} = \delta_v \Delta_{\mathcal{S}} v + f_v(u, v), \quad (5.1)$$

where u and v are the activator and inhibitor respectively, and

$$f_u(u, v) := \alpha u (1 - \tau_1 v^2) + v (1 - \tau_2 u), \quad f_v(u, v) := \beta v \left(1 + \frac{\alpha \tau_1}{\beta} uv \right) + u (\gamma + \tau_2 v).$$

By tuning the parameters, different patterns appear in the steady state solution. As a demonstration, we use parameters in Table 5.1 and set $\delta_u = 0.516\delta_v$ for these simulations. The initial condition is generated by some uniformly random values between -0.5 and 0.5 in a thin strip around the equator of the surface and zeros elsewhere. The reaction diffusion equation is first semi-discretized by the implicit-explicit SBDF2 method in [3, 32]. The idea is to solve the reaction term explicitly and

surface	Pattern	δ_v	α	β	γ	τ_1	τ_2
CDP	spots	1.5×10^{-3}	0.899	-0.91	-0.899	0.02	0.2
	stripes	2.1×10^{-4}	0.899	-0.91	-0.899	3.5	0
Torus	spots	2.3×10^{-3}	0.899	-0.91	-0.899	0.02	0.2
	stripes	8.87×10^{-4}	0.899	-0.91	-0.899	3.5	0
Cyclide	spots	2.2×10^{-2}	0.899	-0.91	-0.899	0.02	0.2
	stripes	8.0×10^{-3}	0.899	-0.91	-0.899	3.5	0
Orthocircle	spots	3.8×10^{-2}	0.899	-0.91	-0.899	0.02	0.2
	stripes	9.0×10^{-4}	0.899	-0.91	-0.899	3.5	0

TABLE 5.1

Example 3. Parameters for Turing patterns.

handle diffusion implicitly. With $\Delta t = 0.05$, we solve the resulting modified Helmholtz equations by applying our Method 4 with around 5000 points on each surface. We run our simulations on the following implicit surfaces: a constant distance product (CPD) surface⁴, a torus⁵, a cyclide⁶ and an orthocircle⁷. We terminate the time evolution at $T = 400$ and $T = 6000$ respectively for the Turing spot and stripe pattern. The results are given in Figure 6.1.

We end this section with some *spiral wave* simulations of the Fitzhugh-Nagumo equation [4] in the form of (5.1) with

$$f_u(u, v) := \frac{1}{\alpha}u(1-u) \left(u - \frac{v+b}{a} \right), \quad f_v(u, v) := u - v.$$

on the torus and CDP surfaces. In this context, u and v represent some chemical concentrations or membrane potential and current. Using $\alpha = 0.02$, $a = 0.75$, $b = 0.02$, $\delta_v = 0$ and the initial condition

$$u(0, \mathbf{x}) = \frac{1}{2}(1 + \tanh(2x + y)), \quad v(0, \mathbf{x}) = \frac{1}{2}(1 - \tanh(3z)).$$

We solve the reaction diffusion equation by SBDF2 with a time step of $\Delta t = 0.02$. Using the values of u or v , we can construct spiral waves by assigning red to $u = 1$, blue to $u = 0$, and interpolate the color in-between. The approximated solution by Method 4 to u gives the spiral waves in Figure 6.2.

6. Conclusion. This work aims to give the first theoretical study for kernel-based embedding methods for surface PDEs. By carefully applying the recently available inverse inequalities on some meshfree trial spaces, we derive a convergent formulation of meshfree embedding method for second order elliptic PDEs on surfaces. The proposed method is easy to implement; it is identical to its domain-type counterpart plus some embedding and stability conditions. Our convergence analysis, which is carried out in the embedding domains, ensures that the proposed method converge at an $m - k - 1/2$ rate in $\mathcal{H}^k(\mathcal{S})$ if a reproducing kernel of $\mathcal{H}^m(\mathbb{R}^d)$ is employed and some smoothness assumptions are satisfied. Most of these assumptions are standard

⁴ $\sqrt{(x-1)^2 + y^2 + z^2} \sqrt{(x+1)^2 + y^2 + z^2} \sqrt{x^2 + (y-1)^2 + z^2} \sqrt{x^2 + (y+1)^2 + z^2} - 1.1 = 0$.

⁵ $(1 - \sqrt{x^2 + y^2})^2 + z^2 = 1/9$.

⁶ $(x^2 + y^2 + z^2 - d^2 + b^2)^2 - 4(ax + cd)^2 - 4b^2y^2 = 0$ with $a = 2, b = 1.9, d = 1, c^2 = a^2 - b^2$.

⁷ $((x^2 + y^2 - 1)^2 + z^2)((y^2 + z^2 - 1)^2 + x^2)((z^2 + x^2 - 1)^2 + y^2) - c_1^2(1 + c_2(x^2 + y^2 + z^2)) = 0$ with $c_1 = 0.075, c_2 = 3$.

for high order convergence except those on the kernel smoothness m and the denseness of the collocation points, which are a direct consequence of the hybrid-type inequalities in our proof. Thus, we present convincing numerical results to show that the theoretical assumptions are sufficient, but not necessary, conditions for convergence. Moreover, after taking both accuracy and efficiency into consideration, a reduced system with some linear ratios of oversampling is recommended for practical use. When the surface of interest has large mean curvature, we can see a clear advantage of this reduce system over an interpolation-based projection method. The successful simulations of various pattern formations further demonstrate the robustness of unsymmetric meshfree collocation methods.

Acknowledgements. This work was partially supported by a Hong Kong Research Grant Council GRF Grant, a Hong Kong Baptist University FRG Grant, and the National Natural Science Foundation of China (11528205).

REFERENCES

- [1] R. Arcangeli, M. C. L. de Silanes, J. J. Torrens, An extension of a bound for functions in Sobolev spaces, with applications to (m, s)-spline interpolation and smoothing, *Numer. Math.* 107 (2) (2007) 181–211.
- [2] R. Arcangeli, M. C. L. de Silanes, J. J. Torrens, Extension of sampling inequalities to Sobolev semi-norms of fractional order and derivative data, *Numer. Math.* 121 (3) (2012) 587–608.
- [3] U. M. Ascher, S. J. Ruuth, B. T. Wetton, Implicit-explicit methods for time-dependent partial differential equations, *SIAM J. Numer. Anal.* 32 (3) (1995) 797–823.
- [4] D. Barkley, A model for fast computer simulation of waves in excitable media, *Physica D: Nonlinear Phenomena* 49 (1) (1991) 61–70.
- [5] R. Barrio, C. Varea, J. Aragón, P. Maini, A two-dimensional numerical study of spatial pattern formation in interacting Turing systems, *Bulletin of mathematical biology* 61 (3) (1999) 483–505.
- [6] M. D. Buhmann, Radial basis functions: Theory and implementations, vol. 12 of Cambridge Monographs on Applied and Computational Mathematics, Cambridge University Press, Cambridge, 2003.
- [7] Y. Chen, C. B. Macdonald, The closest point method and multigrid solvers for elliptic equations on surfaces, *SIAM J. Sci. Comput.* 37 (1) (2015) A134–A155.
- [8] K. C. Cheung, L. Ling, S. Ruuth, A localized meshless method for diffusion on folded surfaces, *J. Comput. Phys.* 297 (2015) 194206.
- [9] K. C. Cheung, L. Ling, R. Schaback, H^2 -convergence of least-squares kernel collocation methods (SINUM, in revision. 2016).
- [10] Z. Ding, A proof of the trace theorem of Sobolev spaces on Lipschitz domains, *Proc. Amer. Math. Soc.* 124 (1996) 591–600.
- [11] G. E. Fasshauer, Meshfree approximation methods with Matlab, *Interdisciplinary Mathematical Sciences* 6. Hackensack, NJ: World Scientific., 2007.
- [12] E. J. Fuselier, G. B. Wright, Scattered data interpolation on embedded submanifolds with restricted positive definite kernels: Sobolev error estimates, *SIAM J. Numer. Anal.* 50 (3) (2012) 1753–1776.
- [13] E. J. Fuselier, G. B. Wright, A high-order kernel method for diffusion and reaction-diffusion equations on surfaces, *J. Sci. Comput.* 56 (2013) 535–565.
- [14] P. Giesl, H. Wendland, Meshless collocation: Error estimates with application to dynamical systems, *SIAM J. Numer. Anal.* 45 (4) (2007) 1723–1741.
- [15] P. Grisvard, Elliptic problems in nonsmooth domains, *Monographs and studies in mathematics*, Pitman Advanced Pub. Program, Boston, London, Melbourne, 1985.
- [16] T. Hangelbroek, F. J. Narcowich, C. Rieger, J. D. Ward, An inverse theorem on bounded domains for meshless methods using localized bases, *ArXiv e-prints*.
- [17] T. Hangelbroek, F. J. Narcowich, C. Rieger, J. D. Ward, An inverse theorem for compact Lipschitz regions in \mathbb{R}^d using localized kernel bases, *ArXiv e-prints*.
- [18] T. Hangelbroek, F. J. Narcowich, X. Sun, J. D. Ward, Kernel approximation on manifolds II: The L^∞ norm of the L^2 projector, *SIAM J. Math. Analysis* 43 (2) (2011) 662–684.
- [19] T. Hangelbroek, F. J. Narcowich, J. D. Ward, Kernel approximation on manifolds I: bounding the Lebesgue constant, *SIAM J. Math. Analysis* 42 (4) (2010) 1732–1760.

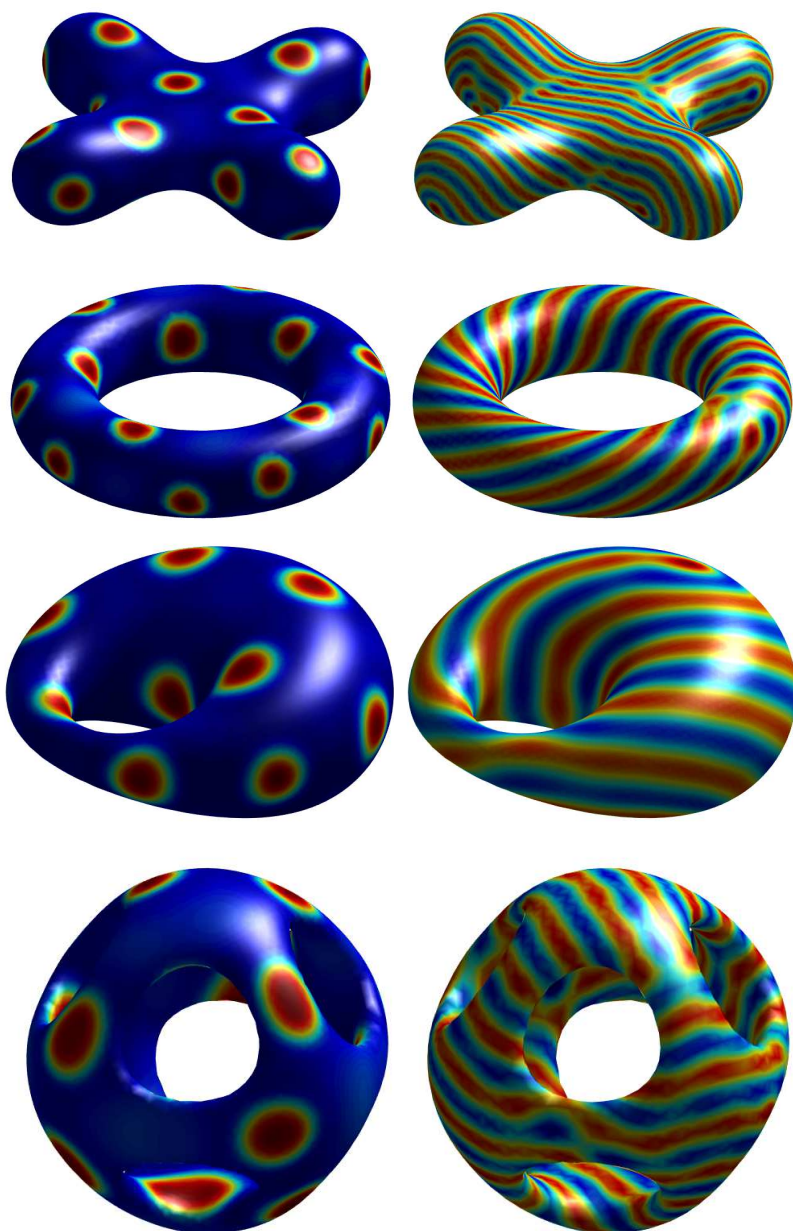


FIG. 6.1. Turing spot and stripe patterns on various implicit surfaces.

- [20] Y. C. Hon, R. Schaback, On unsymmetric collocation by radial basis functions, *Appl. Math. Comput.* 119 (2-3) (2001) 177–186.
- [21] E. J. Kansa, Multiquadrics—a scattered data approximation scheme with applications to computational fluid-dynamics. I. Surface approximations and partial derivative estimates, *Comput. Math. Appl.* 19 (8-9) (1990) 127–145.
- [22] E. J. Kansa, Multiquadrics—a scattered data approximation scheme with applications to computational fluid-dynamics. II. Solutions to parabolic, hyperbolic and elliptic partial differential equations, *Comput. Math. Appl.* 19 (8-9) (1990) 147–161.

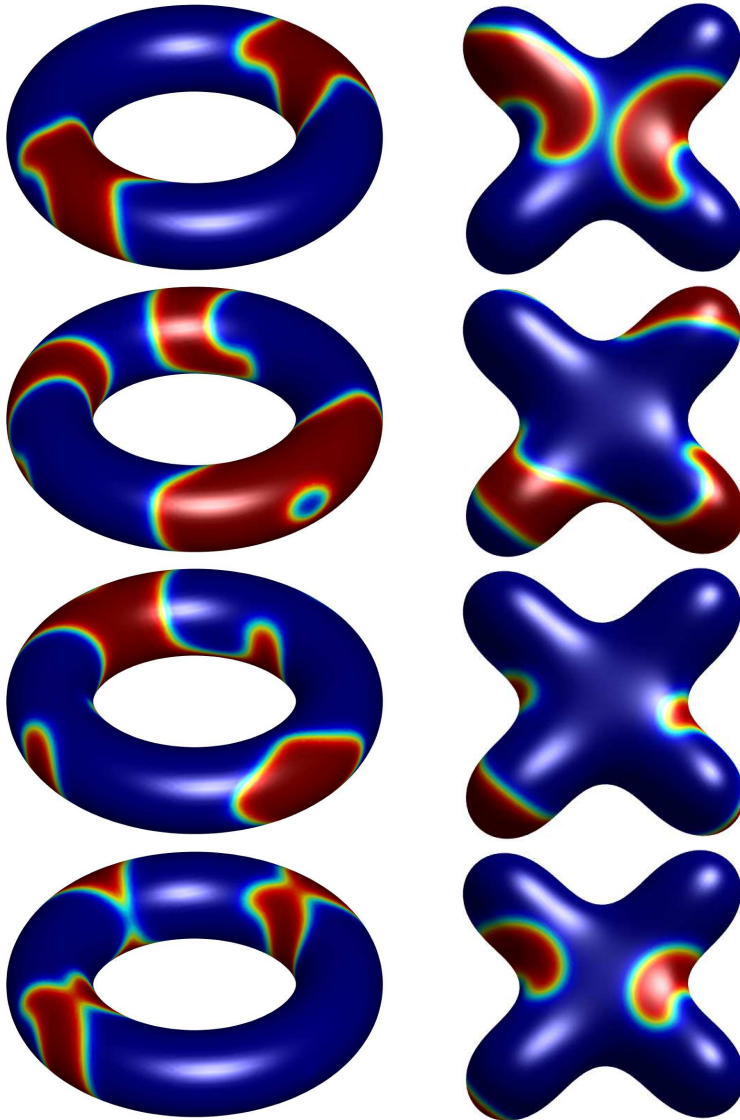


FIG. 6.2. Snapshots of the spiral wave on two different surfaces at various times $t = 4, 5.6, 6.4$ and 7 .

- [23] D. I. Ketcheson, C. B. MacDonald, S. J. Ruuth, Spatially partitioned embedded Runge-Kutta methods, *SIAM J. Numer. Anal.* 51 (5) (2013) 2887–2910.
- [24] C. B. Macdonald, J. Brandman, S. J. Ruuth, Solving eigenvalue problems on curved surfaces using the closest point method, *J. Comput. Phys.* 230 (22) (2011) 7944–7956.
- [25] C. B. Macdonald, S. J. Ruuth, The implicit closest point method for the numerical solution of partial differential equations on surfaces, *SIAM J. Sci. Comput.* 31 (6) (2009) 4330–4350.
- [26] W. R. Madych, An estimate for multivariate interpolation II, *Journal of approximation theory* 142 (2) (2006) 116–128.
- [27] F. J. Narcowich, J. D. Ward, H. Wendland, Sobolev bounds on functions with scattered zeros, with applications to radial basis function surface fitting, *Math. Comp.* 74 (250) (2005) 743–763.
- [28] F. J. Narcowich, J. D. Ward, H. Wendland, Sobolev error estimates and a Bernstein inequality

- for scattered data interpolation via radial basis functions, *Constr. Approx.* 24 (2) (2006) 175–186.
- [29] C. Piret, The orthogonal gradients method: A radial basis functions method for solving partial differential equations on arbitrary surfaces, *J. Comput. Phys.* 231 (14) (2012) 4662–4675.
 - [30] C. Rieger, B. Zwicknagl, R. Schaback, Sampling and stability, in: M. Dæhlen, M. Floater, T. Lyche, J.-L. Merrien, K. Mørken, L. Schumaker (eds.), *Mathematical Methods for Curves and Surfaces*, vol. 5862 of *Lecture Notes in Computer Science*, 2010.
 - [31] I. Rozada, S. J. Ruuth, M. J. Ward, The stability of localized spot patterns for the Brusselator on the sphere, *SIAM J. Appl. Dynamical Systems* 13 (1) (2014) 564–627.
 - [32] S. J. Ruuth, Implicit-explicit methods for reaction-diffusion problems in pattern formation, *J. Math. Biology* 34 (2) (1995) 148–176.
 - [33] S. J. Ruuth, B. Merriman, A simple embedding method for solving partial differential equations on surfaces, *J. Comput. Phys.* 227 (3) (2008) 1943–1961.
 - [34] R. S. Strichartz, Analysis of the Laplacian on the complete Riemannian manifold, *J. Funct. Anal.* 52 (1983) 48–79.
 - [35] C. Varea, J. Aragon, R. Barrio, Turing patterns on a sphere, *Physical Review E* 60 (4) (1999) 4588.
 - [36] H. Wendland, Error estimates for interpolation by compactly supported radial basis functions of minimal degree, *J. Approx. Theory* 93 (2) (1998) 258–272.
 - [37] H. Wendland, *Scattered data approximation*, vol. 17 of *Cambridge Monographs on Applied and Computational Mathematics*, Cambridge University Press, Cambridge, 2005.
 - [38] J. Wloka, *Partial Differential Equations*, Cambridge University Press, 1987.
 - [39] G. Yao, Siraj-ul-Islam, B. Sarler, A comparative study of global and local meshless methods for diffusion-reaction equation, *Comput. Model. Eng. Sci.* 59 (2) (2010) 127–154.
 - [40] N. Yoshida, Sobolev spaces on a Riemannian manifold and their equivalence, *J. Math. Kyoto Univ.* 32 (3) (1992) 621–654.
 - [41] X. Zhang, X. An, C. S. Chen, Local RBFs based collocation methods for unsteady Navier-Stokes equations, *Adv. Appl. Math. Mech.* 7 (4) (2015) 430–440.